C.P. No. 737

C.P. No. 737

MINISTRY OF AVIATION

AERONAUTICAL RESEARCH COUNCIL

CURRENT PAPERS

Experimental Evidence on the Drag at Zero Lift on a Series of Slender Delta Wings at Supersonic Speeds, and the Drag Penalty due to Distributed Roughness

by

M. C. P. Firmin

LONDON: HER MAJESTY'S STATIONERY OFFICE

1964

PRICE 18s 6d NET

U.D.C. No. 533.693.3 : 533.6.013.12 : 533.6.011.5

C.P. No. 737

February, 1963

EXPERIMENTAL EVIDENCE ON THE DRAG AT ZERO LIFT ON A SERIES OF SLENDER DELTA WINGS AT SUPERSONIC SPEEDS, AND THE DRAG PENALTY DUE TO DISTRIBUTED ROUGHNESS

by

M.C.P. Firmin

SUMMARY

Measurements have been made of the drag at zero lift on a series of low drag delta wings of diamond cross-section, with and without distributed roughness.

After allowance has been made for the skin friction, wave drag factors obtained have been compared with theoretical estimates. It is shown that thin-wing theory gives reasonably reliable estimates for the wave drag factor (K_o) but that it tends to overestimate the change in drag as the trailing edge slope is increased.

Slender body theory should not be relied upon to calculate the zero lift wave drag factors since in the region of the trailing edge the assumption of slenderness $\{|\beta^2 \phi_{xx}| << |\phi_{yy}| + |\phi_{zz}|\}$ is only valid for a very restricted range of wings.

Replaces R.A.E. Tech. Note No. Aero 2871 - A.R.C. 24843.

LIST OF CONTENTS

LIST OF TABLES

LIST OF ILLUSTRATIONS

LIST OF ILLUSTRATIONS (Continued)

1 INTRODUCTION

Aerodynamic investigations aimed at the design of large transport aircraft to cruise at supersonic speeds include the search for sharp-edged delta-like wings with subsonic leading edges which have low drag, in particular, a low volume-dependent wave drag. Although other considerations make it likely that the planform of such an aircraft would have streamwise tips and that its cross-section would bulge along the centre-line, some particular problems can be investigated on simpler shapes such as delta wings, with diamond cross-sections, for which theoretical calculations and model manufacture can be more easily accomplished.

The zero-lift drag coefficient for a wing in supersonic flow is usually assumed to be made up of three parts, viz, wave drag, friction drag, and viscous form drag. The volume-dependent wave drag is the drag of the wing in invisid flow, the friction drag is due to the shear stress at the surface, and the viscous form drag is the pressure drag associated with the presence of a boundary layer.

In supersonic wind tunnel investigations, a direct measurement of the wave drag cannot readily be obtained since the viscous form drag cannot easily be separated from it. It is usual to measure the total form drag and compare this with the calculated wave drag.

The wave drag of the wings to be investigated here has been studied theoretically by Weber[1] and Smith and Thomson[2]. Two theories have been used, thin-wing theory and slender-body theory; whereas the former makes the assumption of thinness but not slenderness the latter makes the assumption of slenderness. The further assumption of thinness in the slender theory does not affect the results for the wings being considered, so any difference between the theoretical results may be primarily attributed to a violation of the slenderness assumption. These theories are based on the assumption of an invisid flow and one object of the present tests is, therefore, to look for any indication of possible effects of viscosity. Further, the theories are based on the linearised equations of motion for supersonic flows; hence another object of the tests is to look for any deviations that may be interpreted as having been caused by non-linear, such as transonic, phenomena.

The most direct measurement of the total form drag is from the integration of detailed pressure measurements over the wing surfaces. This method is tedious and, since relatively large models are required, can only be used in large wind tunnels. A less direct determination of the total form drag is to measure the total drag and make an allowance for the friction drag. The absolute magnitude of the total form drag will then be in doubt due to uncertainties in the estimation of the skin friction, but the method is suitable for comparing wave drags on wings of the same planform with different thickness distributions.

The present investigation uses the indirect method for the determination of the total form drag and covers the measurement of the total drag at zero lift on a series of delta wings, with diamond cross-sections and with volume distributions which progressively become geometrically less smooth and less slender.

2 DESCRIPTION OF THE MODELS

2.1 Design

All the wings are of delta planform and have an aspect ratio of unity, unswept trailing edge, diamond cross-sections and equal volume ($\tau = {}^{V}/(Sc_o)^{3/2} = 0.05$). The wings are then completely defined by the cross-sectional area distribution, which for the models of these tests is given by

$$\frac{S(\xi)}{c_o^2} \Big/ \frac{V}{c_o^3} = \xi^2 (1 - \xi) \sum_{0}^{3} An\, \xi^n \qquad (1)$$

where $\xi (\equiv {}^{x}/c_o)$ is the chordwise station as a fraction of the centre line chord and is measured from the apex. The coefficients An are given in Table 1 and the distributions of the cross-sectional area and of the thickness at the centre line for all wings are given in Figs.1 and 2.

Wings 1 to 4 form a series with progressively steeper slopes at the trailing edge, obtained by rather localised bulges in the region of the trailing edge. Each gives within this particular family of wings a minimum value of the wave drag, by slender body theory, for a particular value of the first derivative of the cross-sectional area at the trailing edge [$S'(1)$] and for $\beta S/c_o = 0.4$. The wave drag, calculated by thin-wing theory, is also close to a minimum and all the values, according to both approximations, lie close to their respective lower-bound envelopes for this particular family of shapes (see Ref.1). But the actual values from the two theories differ more and more from one another as the slope at the trailing edge increases, those from slender body theory being the lower. All four of these wings have their maximum cross-sectional areas at about half the length of the wing.

The other two wings of the series (wings E and G) were investigated in Ref.2. Both are reasonably geometrically smooth but the position of the maximum cross-sectional area is further aft, i.e. at 65% and 75% of the length of the wing for wing E and G respectively. They belong to the same family of wings as the first series and both give minimum values of the wave drag by thin-wing theory for the particular locations of the maximum cross-sectional area and for $\beta S/c_o = 0.6$. These minimum values lie again close to the lower-bound envelope and the general drag values stay near this envelope even much lower values of $\beta S/c_o$.

2.2 Construction

The first four models (wings 1 to 4) were constructed of steel plate with a centre-line template and the regions between the template and the leading edges filled with araldite. The nose tip, and the region near the

trailing edge have steel surfaces (Fig.5). This method of construction was attempted in an effort to avoid some tangent-plane grinding and so reduce the time required for manufacture. This technique failed to improve on existing methods since, the main steel plate and template distorted when the araldite was applied, and some cracking of the araldite occurred in the later stages of manufacture. Wing E was constructed of steel and ground by the tangent-plane method, with the final finishing completed by hand. Wing G was roughed out in steel but had a thin layer (approximately 0.02" thick) of araldite forming the surface. This method worked extremely well since the araldite was easier to machine and the time involved in final handwork was reduced. It should, however, be pointed out that, although the method is suitable for models where only small lift forces are to be measured, it may not be suitable for other models due to a loss of strength near the wing tips.

All the wings, which were 12 inches long, have a thin circular sting which modifies the area distribution over the last 12% of the centre-line chord but modifies only about 1% of the surface area. The sting diameter is 5% of the wing span. All the planform edges of the models had a nominal 0.002 inch radius and the thickness distributions were modified to include this small extra thickness.

The wings were mounted on a special support which incorporated a form of chuck for holding the model sting. The chuck was mounted on the front end of a twin cantilever type of strain gauged drag balance. The balance also had extra strain gauges on the cantilevers for the determination of the zero-lift condition. The stings were extremely flexible. An extra model "steady" was therefore incorporated for use when starting and stopping the wind tunnel, and also for use at high stagnation pressures if the model started to oscillate. The extra steady took the form of a tube which was supported on bearings and could be traversed forward to steady the model in about 3 seconds. Fig.3 shows photographs of one of the wings mounted in the wind tunnel. The right hand photograph shows the steady in the forward position supporting the model on spring loaded rubber pads. Limit switches and a solid stop avoid the balance being overloaded.

3 EXPERIMENTAL EQUIPMENT AND ACCURACY

3.1 Wind tunnel

The models were mounted in the R.A.E. No.19 (18" x 18") supersonic wind tunnel which is a continuous return-flow closed-circuit tunnel with a nominal Mach number range of 1.4 to 2.2 with a square working section 18 inches wide at all Mach numbers. In the present tests the stagnation pressure was varied up to a maximum of 60 inches of mercury corresponding to a maximum Reynolds number of 9×10^6 based on the wing centre line chord*.

The stagnation temperature was kept constant for all tests at a particular Mach number such that the model remained close to normal temperature (15°C)

---

* The limitation on stagnation pressure was determined by sting strength since at pressures higher than 60 inches of mercury it was found that the model oscillated more than could be permitted. The wind tunnel could otherwise be run at stagnation pressures up to 84 inches of mercury.

except for tests at Reynolds numbers less than about 2×10^6 where it was found that the stagnation temperature dropped even with the tunnel cooler fully closed.

The tunnel air was kept dry during these tests using a dry-air interchange system. The tunnel humidity was measured during the tests and no results were recorded until the humidity was less than 0.0002 lb of water per lb of dry air.

3.2 Accuracy

3.2.1 Tunnel flow

The supersonic nozzles used for these tests are all double sided and the Mach number distribution has been obtained but not the flow inclination. The Mach number distributions along the centre line of the tunnel where the model is situated are given in Fig.4. The changes of the Mach number are reasonably gradual over the region occupied by the model and are within the following limits:-

$$M = 1.40 \pm 0.010$$
$$M = 1.58 \pm 0.012$$
$$M = 2.01 \pm 0.020$$
$$M = 2.19 \pm 0.008$$

However, these changes are large enough to affect the drag measurements which are susceptible to errors due to the consequential changes of the static pressure along the axis of the tunnel (buoyancy effect). It is shown in Appendix 1 how the resulting correction to the drag coefficient can be calculated under the assumption that the static pressure gradient is constant. The changes allowed for, in the present tests, are given by the dashed lines in Fig.4 and the following corrections have been applied to all the measured drag results:-

$$M = 2.01 \qquad -\Delta C_{D_o} = -0.00048$$
$$M = 2.19 \qquad -\Delta C_{D_o} = +0.00012$$

No correction for $M = 1.40$ and 1.58.

3.2.2 Measurements

Estimates of the accuracy of the measurements made by the strain gauged balance suggest that over the test Mach number range and at the highest Reynolds numbers tested ($Re = 8 \times 10^6$) the errors in the drag coefficients are within the following limits:-

$$\pm 0.00005 \pm 0.004 C_{D_o}$$

To obtain corresponding figures for lower Reynolds numbers this value should be increased by the ratio of the Reynolds numbers.

The drag results have been adjusted by the application of an increment corresponding to the difference between the measured base pressure and that of the free stream acting over the sting base area, so that the base pressure coefficient is zero. When wave drag factors (K_o) are deduced a further allowance is made for the influence of the sting on the pressure field over the rear of the wing (see para.7.2).

4 EXPERIMENTAL TECHNIQUES

The results of many wind tunnel tests, like the present series, are analysed by estimating the amount of skin friction drag contained in the overall drag, according to some established theoretical method. This presupposes that the state of the boundary layer is known. Under wind tunnel conditions, and dependent upon the Reynolds number, turbulence level of the stream and the shape of the model, the boundary layer is normally found to be laminar over some part of the wing; this is followed by a transition region of finite streamwise extent and finally by a fully turbulent layer. The extent of these regions is difficult to observe; for instance, most techniques for indicating transition would seem to indicate neither where the layer ceases to be laminar nor where the layer becomes truly turbulent but some point in between. And even if these regions were sufficiently well known, there exists no method which can cope with so complicated a boundary layer flow, especially if the transition region takes up an appreciable portion of the wing chord as it is likely to do on relatively small models. It is, therefore, preferred to make the boundary layer wholly turbulent by artificial means such as roughness bands. This has the added advantage when testing aircraft models that the method for estimating the skin friction can be the same for the model and for the full-scale aircraft, if the latter can be assumed to have a fully turbulent boundary layer. The application of roughness bands to force transition introduces, however, its own problems and these are investigated in some more detail in the present tests in which relatively small models are used at Reynolds numbers which are not unduly small.

4.1 Transition bands

It is well known that distributed roughness is an efficient method of changing the transition pattern on a wing, and, provided the grain size is large enough, non-laminar boundary-layer flow can occur at or very close* to the distributing elements[3,4,5]. The grains themselves can, however, disrupt the boundary layer such that a truly turbulent layer does not occur until further downstream. It is not known what influence this has on the skin friction.

Particularly in small supersonic wind tunnels the grain size required to provide a non-laminar boundary layer can be such that the drag of the transition band is significant compared with the drag being measured. It is then essential to be able to eliminate any drag due to the grains which is not associated with changing the boundary layer to a truly turbulent one.

---

* There is some evidence that for single roughness elements there is a minimum distance behind the roughness at which transition begins to take place[6].

Normal techniques for applying grains to the surface of a model by means of adhesives which harden, call for a fire-control spray gun, and an experienced operator[7]; even then it is very difficult, if not impossible, to ensure an even coverage with the correct distribution each time the grains are applied. It was therefore decided to see if instead some simple technique could be found.

The transition bands must have the following properties if reliable and repeatable results are to be obtained in a reasonable time.

(1) Simple to apply.

(2) Uniform and repeatable coverage.

(3) Grains must not be blown off during the experiment.

(4) It must be possible to estimate the drag due to the grains which is not associated with changing the boundary layer to a truly turbulent one.

A simple transition band was obtained which satisfied conditions (1) and (2) above by using double sided sellotape marketed by Gordon and Gotch (Sellotape) Limited of London, E.C.2. The technique was to stick the tape onto a metal plate, remove the separating tape, and then sprinkle carborundum of the required grain size onto the tape*. In order to obtain consistent coverage, it was found necessary to saturate the area with carborundum and then brush off the surplus.

The mean grain sizes used were obtained by hand sieving the carborundum and computing the mean height of a single layer of grains (air gaps not included) uniformly distributed on the surface.

The band was wrapped round the leading edge of the model since it was felt that this was preferable to having two bands with a step at the beginning of each. A possible disadvantage of the method is the excessive thickness of the tape (0.002 inches) and its associated layers of glue (about 0.001 inches each). A check was made which showed the increase in drag due to the band alone (i.e. change in wave drag and change in skin friction drag) was negligible at the highest Reynolds number tested. At lower Reynolds numbers the change in drag was significant but may be attributed, at least partially, to a change in the skin friction drag**.

Fig.5 shows wing 2 with transition bands (mean grain height 0.0038 inches) wrapped round the leading edges and Fig.6 gives photomicrographs of specimen roughness bands. The width of the band on each side of the wing was 0.25 inches.

---

* Carborundum is probably not the best type of roughness element to use since its irregular shape makes it difficult to determine the mean grain size. Uniform glass balls (ballontini) are now available from English Glass Co. Ltd, of Leicester.

** See Fig.7(b) for results.

Inspection of the models before and after test confirmed that very few grains were blown off the transition bands during testing, so that condition (3) above was fulfilled. Discussion of the requirements of the last condition stated above will be left until the results are discussed as a whole in section 6.1.

5 PRESENTATION OF THE RESULTS

Results have been obtained for each wing tested with free transition and with up to four transition bands of different grain sizes. The results are given in Figs.7, 8 and 9 in terms of the drag coefficient based on plan area.

The results were obtained at various Reynolds numbers for each transition band but curves at constant Reynolds number have also been drawn. The wings and the Mach numbers at which they have been tested are given in the chart below.

Mach Number \ Wing	1	2	3	4	E	G
1.4			X		X	
1.58			X		X	
2.01	X	X	X	X	X	X
2.19			X		X	

6 DISCUSSION OF RESULTS AND ANALYSIS

6.1 Discussion

All the results (Figs.7 to 9) where transition bands have been used have a characteristic shape for the change in drag with Reynolds number. It would appear that as the Reynolds number is reduced the skin friction drag coefficient first of all increases and then decreases rapidly. This is what would be expected if the boundary layer changed fairly rapidly from a fully turbulent condition to one in which quite a large area of laminar flow occurs behind the disturbing elements. The same form of change in drag with Reynolds number has been found by Mabey[8].

Curves at constant Reynolds number have also been drawn, but their shape is not well defined for small grain sizes. It has, however, been found that within quite close limits the variation of drag at constant Reynolds number is linear for large enough grain sizes. The information published on the grain size required for non-laminar boundary layer flow at, or very close to, the disturbing elements[3,4,5] is not at all consistent, but covers the values suggested here by the departure of the curves at constant

Reynolds number from a linear variation with grain size. The work of Luther[4] on bodies using roughness on the nose only, gives results consistent with those obtained here, except, that in Ref.4 there was no measurable increase in drag with grain size above some critical grain size, which suggests that the linear increase in drag measured here is directly attributable to the drag on the grains. The critical Reynolds numbers obtained from the trends of the present results at constant Reynolds number (Table 2) are larger than those suggested by the form of the curve at constant grain size. It may therefore be misleading to assume that the boundary layer is sufficiently disturbed, to obtain a fully non-laminar boundary layer, as soon as the drag coefficient starts to decrease on increasing the Reynolds number.

It is surprising that the change in drag with grain size is linear for large enough grain sizes, since it is probably made up in three parts, viz. the pressure drag of the grains, the distortion of the profile due to the presence of the grains and any excessive change in the boundary layer not associated with making it truly turbulent. It is not known what proportion of the increase in drag is due to the wave drag of the grains, but this could account for a large part of it since the theoretical maximum momentum that could be destroyed by the grains is about twice the measured drag increment. The maximum was obtained by assuming the stagnation pressure behind a normal shock acted over a step of the same height as the transition band. Any detailed dimensional analysis to show whether, or not, a linear increase in drag due to the form drag on the grains would be expected seems to be prejudiced by the underlying assumption, that must be made, about the flow over the grains and the interference between them. One simple idea, that the momentum destroyed by the band will be proportional to the band height (i.e. grain size) does, however, give the required result. Fig.10 gives a typical curve of drag coefficient against grain size at a Reynolds number of 4×10^6 for wing 2. This curve shows all the characteristics mentioned above.

6.2 Analysis

The results of Fig.10 also suggest that the zero lift drag coefficient for the wing with a truly turbulent boundary layer will certainly be higher than the free transition value (A), since for this point it is known that at least part of the boundary layer was laminar; and it will probably be lower than the value at which the linear part of the curve commences (B), since at this point it is thought that the boundary layer is fully non-laminar, but that the drag should include a contribution from the grains.

Without further evidence of the influence of the grains on the boundary layer it is not possible to put closer bounds on the drag coefficient for the wing with a truly turbulent boundary layer. It is, however, possible to analyse the results further if it is assumed that the contribution to the drag from the presence of the grains, not associated with making it truly turbulent is predominantly form drag, and is either small or has a linear dependence on the grain size, and is thus removable by extrapolation. It may, however, be argued that at some small grain size the form drag on the grains would not be linear with grain size since the grains are becoming small compared with the boundary layer thickness. But since the grains exist right up to the leading edge the boundary layer should have only a small effect on the authenticity of the extrapolation.

Further indirect evidence supporting the method of extrapolation is that the wave drag factors obtained (see para.7.3) are almost independent of Reynolds number. Any incorrect extrapolation would have shown as an apparent increase in wave drag factor as the Reynolds number was increased since the boundary layer thickness is dependent on Reynolds number.

6.3 Derived results

It cannot be proved that $\left(C_{D_o}\right)_T$ (Fig.10) is a good approximation to the drag coefficient for the wing with a truly turbulent boundary layer, but at the moment no better approximation exists so all the results obtained have been analysed in terms of it. But it may reasonably be assumed that the error introduced by this method is not substantially larger than the difference between this extrapolated value and that corresponding to point B in Fig.10. For a Reynolds number of 8×10^6 this is only about 3% of the overall drag because the grain size needed to produce a fully non-laminar layer is not very large. Hence this method of extrapolation can be used without introducing inadmissible errors in such cases where the Reynolds number is large enough for relatively small roughnesses to produce a non-laminar layer. If however the Reynolds number and the model size are relatively small and the grain size needed relatively large, then the uncertainties involved may become excessive. In general, only direct measurements of the skin friction through the transition region can reduce this uncertainty.

Results derived by this method at all the Mach numbers at which tests were made are given for wing 3 and wings E in Fig.11. Fig.12 gives results for all the wings at a Mach number of 2.01. At the lower Reynolds numbers the form of the curves at constant Reynolds numbers (Figs.7, 8 and 9) are not well defined since it is not clear where the linear region starts for extrapolation. At these Reynolds numbers the full lines have been obtained by assuming that the results for the two largest grain sizes are on the linear part of the curve, and the dashed lines by using only the point on the largest grain size curve and the trend of the results at higher Reynolds numbers. The latter method will probably give more reliable results since it is probable that only the results for the largest grain size have a fully non-laminar boundary layer (see Table 2).

7 DETERMINATION OF THE ZERO LIFT WAVE DRAG FACTOR (K_o)

The zero lift wave drag factor (K_o) for a slender wing is defined[10] as being the ratio of the wave drag of the given configuration and the wave drag of a Sears-Haack body of the same length and volume.

i.e.

$$K_o = \left(C_{D_o}\right)_w \times \frac{\pi\left(\frac{S}{c_o}\right)}{128\left(\frac{v}{c_o^3}\right)^2} \qquad (2)$$

As stated earlier, to obtain the wave drag factor from drag measurements it is necessary to be able to estimate the contribution of the skin friction, which will, for free transition results, also require a knowledge of the transition process. It is usual to neglect the contribution from the viscous form drag in the analysis, but it should be pointed out that influence of the boundary layer on the form drag may be as high as 4% of the wave drag at the Reynolds numbers of the test*.

7.1 Estimation of the skin friction drag coefficient

7.1.1 Fully turbulent boundary layer

An estimation of the skin friction on a three dimensional delta wing with a fully turbulent boundary layer is not yet possible unless some simplifying assumptions are made. The simplifying assumptions used here are that strip-theory holds, so that two-dimensional results may be used; that the wing approximates to a flat plate; and that the increase in surface area above that for a flat plate may be covered by a simple factor.

Two methods of estimation have been used. The first method was suggested for two-dimensional flat plates in compressible flow by Monaghan[11] as being a simple formula to use. It is derived from incompressible results and uses the Blasius formula:-

i.e.
$$C_F = 0.074\ Re^{-1/5} \qquad (3)$$

with a compressibility factor. It was pointed out in Monaghan's note that the method would only be expected to give reliable results over a small range of chord Reynolds numbers near 10^7, and that the extension he gives to compressible flow cannot fully be justified.

The method has, however, been used with remarkable success by Courtney and Ormerod[12] and in previous unpublished work at R.A.E. Bedford on slender wings with diamond cross-sections. Good agreement has been obtained between results obtained for K_o by integration of the pressure distribution and derived from drag measurements. In more recent tests by Taylor[13] on a slender "Ogee" wing he found that the method underestimated the skin friction drag by about 10%.

The second method uses the intermediate-enthalpy method suggested by Eckert[14] and Monaghan[15]. It uses as a basis the Prandtl-Schlichting formula,

i.e.
$$C_F = 0.46\ (\log_{10} Re)^{-2.6} \qquad (4)$$

for incompressible flow, which is applicable over a much wider range of Reynolds numbers than the Blasius formula. For compressible flow both Eckert and Monaghan have shown that, over a wide range of Mach numbers and

---

* Unpublished calculations by Professor J.C. Cooke and J.A. Beasley on wing 3 at M = 2.2.

temperatures, a close approximation to the local skin friction and heat transfer, is obtained if the physical properties of the air appearing in the incompressible flow formula are evaluated at a temperature T* corresponding to an enthalpy i* which is intermediate between those corresponding to ambient and surface conditions.

The intermediate-enthalpy method gives a value about 10% lower than the first method for the skin friction coefficient over the range of Reynolds numbers for which tests have been made.

7.1.2 Part-laminar boundary layer

When the boundary layer is partly laminar, as in the case of the free transition results, it is necessary to make further simplifying assumptions about the transition process. Although it is known that transition occurs over a region it has been assumed that transition occurs along some locus on the wing. This locus has been determined by oil flow using titanium oxide mixed with a drop of oleic acid and the oil as described by Stanbrook[16]. The method relies on the surface friction being different in the laminar and turbulent regions. Quite well defined patterns are obtained, a photograph of wing 2 at a Reynolds number of 3.75×10^6 is given in Fig.13. Almost the same locus was obtained by using the azobenzene sublimation technique as described in references 9 and 17.

Having obtained the 'point of transition' for each spanwise strip the momentum thickness was assumed to be continuous at transition. Otherwise the same simplifying assumptions and methods are used as in the case of the fully turbulent boundary layer.

7.2 Effect on K_o of the skin friction estimates

The zero lift wave drag factors (K_o) have been determined for wing 2 using all the above estimates for the skin friction and also making an allowance for the influence of the sting on the pressure field. The allowance was quite small and included the contribution for the rearward-facing wing surface masked by the cylindrical sting and a contribution for the pressure field due to the sting on the rear of the wing. Both these corrections were estimated by linear theory.

The results are given in Fig.14. There is some degree of uncertainty about the absolute magnitude of K_o due to the uncertainty in estimating the skin friction even if the boundary layer is truly turbulent. The free-transition method gives a result in fair agreement with the fully-turbulent boundary layer method, there being only a difference of about 5% in K_o between corresponding methods.

As mentioned previously, the skin friction has been fairly accurately predicted in previous tests in the 8' x 8' supersonic tunnel at R.A.E. Bedford by Monaghan's original methods for Reynolds numbers based on the wing length in the region of 10^7. The only real exception is in Taylor's tests where in this case the intermediate-enthalpy method would have given an even bigger error.

Although Monagham's original method is unlikely to give correct results at Reynolds numbers far removed from 10^7, its use is justified, on past experience, in the present context where zero lift wave drag factors are required.

7.3 Zero lift wave drag factors

7.3.1 Results

The derived zero lift wave drag factors (K_o) are given in Figs.15 and 16 at various Mach numbers for wings 3 and E. In Fig.17 similar results are given for all the wings tested at a Mach number of 2.01. These results have been derived from the results given in Figs.11 and 12 and have the same limitations at low Reynolds numbers as discussed in para.6.3. For the reasons given in the previous section all these results have been obtained using Monaghan's original method for the influence of the skin friction on the results.

The results show very little influence of Reynolds number except perhaps at M = 1.40. At this Mach number the results for wing 3 tend to increase with increasing Reynolds number. This is consistant with a recompression occurring in the central region of the wing near the trailing edge as found during pressure measurements at Mach numbers up to M = 1.40[18,19*] on this wing.

7.3.2 Comparisons with theoretical results

Although some doubt has been cast in the preceding sections about the estimation of the skin friction used in deriving the zero lift wave drag factors, this should not affect the relative changes in K_o that have been measured between the wings of the series, provided the skin friction is the same for all the wings in the series, otherwise changes in skin friction will appear as apparent changes in K_o.

Table 3 gives a summary of all the results obtained at Reynolds numbers of 4×10^6 and 8×10^6. Where more than one value has been obtained at a Reynolds number of 4×10^6 then the results from the dashed curves (Figs.15 to 17) have been used. The theoretical values for K_o have also been given as derived from thin-wing theory and slender-body theory. A further column has been added giving ΔK_o, the difference between the experimental values for K_o and those given by thin-wing theory.

i.e. $$\Delta K_o = K_o \text{ (measured)} - K_o \text{ (thin-wing theory)}$$

The results in Table 3 and Fig.19 indicate that the derived wave drag factors may be estimated fairly accurately by thin-wing theory; the maximum ΔK_o for all the wings over the range of tests was only about 20% of K_o. Slender body theory on the other hand should not be relied upon since the condition of

---

* In the tests reported in references 18 and 19 the wing was supported from the undersurface so that the sting should not influence the measurements.

slenderness, that $\beta^2|\phi_{xx}|$ be small compared with $|\phi_{yy}| + |\phi_{zz}|$, is only achieved on wings with a pressure gradient that decreases to a very small value near the trailing edge. Such a wing has the now well known Lord V area distribution[20]. Wing E of the present series is fairly 'smooth' and both theories give a K_o of the same order, but for the other wings in the series the two theories give completely different values for K_o except when $\frac{\beta S}{c_o} \to 0$.

All wings of the series have the same volume and planform. The four coefficients (equation 1) defining the area distribution have, therefore, been reduced to three independent parameters which, vide eqn.1, define the thickness distribution of the series of models completely. The parameters chosen are $\frac{S'(1)}{c_o} \Big/ \frac{v}{c_o^3}$, $S''(1) \Big/ \frac{v}{c_o^3}$, $S''(0) \Big/ \frac{v}{c_o^3}$ and are given for all the wings in Table 3. Although they are the derivatives of the area distribution at the trailing edge and nose of the wings a change in any one of them represents a change in the area distribution over the whole wing. For the six wings of the series all the parameters defining the wings are different but wing E has nearly the same values for $S''(0)$ and $S''(1)$ as for wing G.

One of the original requirements of these tests was to examine the influence of the trailing edge slope on K_o. A plot has therefore been given of ΔK_o against $\frac{S'(1)}{c_o} \Big/ \frac{v}{c_o^3}$ (Fig.18). Based on the results for the wings for which $S'(1)$ is virtually the only variable (viz. E and G) there is a tendency for ΔK_o to increase with $S'(1)$. The results for wing 4, and perhaps, to a much lesser extent, wing 3, tend to deviate from this trend. These wings have particularly extreme volume distributions (i.e. extreme values for $S''(0)$ and $S''(1)$). The wings of the present series give no information on the variation of ΔK_o with volume parameter (τ) or with the planform shape. Although ΔK_o does not appear to depend significantly on Reynolds number, within the range of tests made, ΔK_o may include some contribution due to any difference in skin friction drag between the wings of the series. (In the analysis it has been assumed that at each Mach number, the skin friction was practically the same for all the wings of the series, no account being taken of the influence of pressure gradients.)

In Fig.19 results are given for K_o at several Mach numbers for wing 3 and wing E at Reynolds numbers of 4×10^6 and 8×10^6. Wing 3 has a much more extreme area distribution (Fig.2) and a much larger slope near the trailing edge than wing E. The results for both wings follow quite closely the same trends as the Mach number is changed except that at $M = 1.4 \left(\frac{\beta S}{c_o} = 0.245\right)$ a marked drop in K_o has occurred for wing 3. As mentioned previously, a recompression has been found to occur in the central region of this wing near the trailing edge at Mach numbers up to 1.4 (see para.7.3.1). The drop in K_o

is consistent with such a recompression. The change in K_o from wing E to wing 3 at the other Mach numbers is not as large as predicted by thin-wing theory; only about half the increase predicted has been measured. The slender-body theory values given on the figure indicate how sensitive this theory is to the condition of slenderness. Wing 3 is obviously not slender.

8 CONCLUSIONS

Analysis of the measurements of the drag at zero lift highlights several problems that need solution before really adequate analysis of the results can be made.

No adequate method exists for the estimation of the skin friction drag coefficient on three dimensional wings with, or without, pressure gradients.

If measurements are made with free transition then not enough is known about the natural transition process, even on flat plates, to enable adequate skin friction estimates to be made.

If attempts are made to fix transition by distributed roughness not enough is known about the influence of the roughness on the boundary layer. It has also been shown that appreciable drag penalties may arise due to the grains.

However, if the Reynolds number and model size are large enough for relatively small grains to produce a non-laminar boundary layer, then a method of extrapolation can be used without making the error inadmissibly large. After such an allowance has been made, and an allowance for the skin friction, it is shown that the remaining drag may be estimated with reasonable accuracy by thin-wing theory. Slender-body theory should not be relied upon to give accurate zero lift wave drag factors.

There is no evidence of any large dependence of the wave drag factors on Reynolds number except for wing 3 at a Mach number of 1.40 where it is known that a form of transonic recompression exists near the wing trailing edge.

On the assumption that the skin friction drag is unaffected, the results also suggest that thin-wing theory tends to overestimate the increase in drag as the trailing edge slope is increased.

Further results for pressures measured on these wings and about the transonic behaviour will be communicated later.

LIST OF SYMBOLS

A_o, A_1, A_2, A_3 = coefficients which determine the shape of the wing (equation 1)

C_{D_o} = measured drag at zero lift

$\left(C_{D_o}\right)_T$ = C_{D_o} for a wing with a fully turbulent boundary layer (Fig.10)

$\left(C_{D_o}\right)_w$ = wave drag coefficient

ΔC_{D_o} = change in drag due to gradual Mach number change along axis of wind tunnel (see appendix)

C_p = pressure coefficient $\left(\frac{P - P_\infty}{q}\right)$

c_o = wing chord at centre line (12.00 inches)

D = total drag

K_o = zero lift wave drag factor (equation 2)

P = local pressure

P_∞ = ambient pressure

q = kinetic pressure of free stream

M = mean free stream Mach number

S = semi span at the trailing edge

$S(\xi)$ = cross sectional area in plane normal to free stream

$S'(\xi)$, $S''(\xi)$ = first and second derivatives of $S(\xi)$ with respect to (ξ)

v = volume of the wing

x, y, z = cartesian co-ordinates with the origin at the apex of the wing; x axis measured in the direction of the undisturbed stream; the z axis normal to the chordal plane of the wing

LIST OF SYMBOLS (Continued)

β = $\sqrt{M^2 - 1}$

ξ = $\frac{x}{c_o}$, the chordwise station as a fraction of the centre line chord and measured from the apex

ϕ = velocity potential

τ = $v/(\text{planform area})^{3/2}$, a volume parameter

LIST OF REFERENCES

No.	Author	Title, etc.
1	Weber, J.	Some notes on the zero lift wave drag of slender wings with unswept trailing edge. A.R.C. R. & M. 3222, December 1959.
2	Smith, J.H.B. Thomson, W.	The calculated effect of the station of maximum cross-sectional area on the wave drag of delta wings. A.R.C. C.P. 606, September 1961.
3	Fallis, W.B.	On distributed roughness as a means of fixing transition at high supersonic speeds. Jnl. Aero Sci. 22 (5), May 1955.
4	Luther, M.	Fixing boundary layer transition of supersonic wind tunnel models. Jnl. Aero Sci. 24 (8), Aug. 1957.
5	Potter, J.L. Whitfield, J.D.	Effects of slight nose bluntness and roughness on boundary layer transition in supersonic flows. Jnl. Fl. Mech. 12 (4), April 1962.
6	Van Driest, E.R. Blumer, C.B.	Boundary layer transition at supersonic speeds - three dimensional roughness effects (spheres). Jnl. Aero Sci. 29 (8), Aug. 1962.

LIST OF REFERENCES (Continued)

No.	Author	Title, etc.
7	Rogers, E.W.E. Hall, I.M. Appendix by Berry, C.J. Townsend, J.F.G.	An investigation at transonic speeds of the performance of various distributed roughness bands used to cause boundary layer transition near the leading edge of a cropped delta half wing. Appendix - A roughness band technique and materials. A.R.C. C.P. 481, May 1959.
8	Mabey, D.G.	Drag penalties due to distributed roughness on slender wings at supersonic speeds. Unpublished M.O.A. Report.
9	Main-Smith, J.D.	Chemical solids as diffusible coating films for visual indication of boundary layer transition in air and water. A.R.C. R. & M. 2755, February 1950.
10	Küchemann, D.	Some considerations of aircraft and their aerodynamics for flight at supersonic speeds. A.R.C. 21102, June 1959.
11	Monaghan, R.J.	Some remarks on choice and presentation of formulae for turbulent skin friction in compressible flow. Unpublished M.O.A. Report.
12	Courtney, A.L. Ormerod, A.O.	Pressure-plotting and force tests at Mach numbers up to 2.8 on an uncambered slender wing of $p = \frac{1}{2}$, $s/c_o = \frac{1}{4}$ ('Handley Page Ogee'). A.R.C. R. & M. 3361, May 1961.
13	Taylor, C.R.	Measurements, at Mach numbers up to 2.8, of the longitudinal characteristics of one plane and three cambered slender 'ogee' wings. A.R.C. R. & M. 3328, December 1961.
14	Eckert, E.R.G.	Survey on heat transfer at high speeds. WADC Technical Report No. 54-70, TIL No. P.49878, April 1954.
15	Monaghan, R.J.	Formulae and approximations for aerodynamic heating rates in high speed flight. A.R.C. C.P. 360, October 1955.
16	Stanbrook, A.	The surface oil flow technique as used in high speed wind tunnels in the United Kingdom. A.R.C. 22385, August 1960.

LIST OF REFERENCES (Continued)

No.	Author	Title, etc.
17	Winter, K.G. Scott-Wilson, J.B. Davies, F.V.	Methods of determination and of fixing boundary layer transition on wind tunnel models at supersonic speeds. A.R.C. C.P. 212, September 1954.
18	Firmin, M.C.P.	The pressure distribution on slender delta wings at supersonic speeds. Unpublished M.O.A. Report.
19	Firmin, M.C.P.	Flow visualization and pressure distribution on a slender delta wing of diamond cross section at transonic speeds. Unpublished M.O.A. Report.
20	Lord, W.T. Green, B.	Some thickness distributions for narrow wings. A.R.C. 19459, February 1957.

APPENDIX

CORRECTION TO C_{D_o} FOR A GRADUAL MACH NUMBER CHANGE ALONG THE AXIS OF THIS WING TUNNEL

If a Mach number gradient exists along the axis of the empty wind tunnel in the region normally occupied by the model then a correction to the drag measurements may be necessary.

Let M be the average value of the Mach number and ΔM be the departure from it; then the increment of drag is

$$\Delta C_{D_o} = 4 \int_o^1 \left[\int_{y/S}^1 \left\{ \frac{\Delta P_\infty}{q} + \frac{\Delta(C_p q)}{q} \right\} \frac{\partial(z/c_o)}{\partial \xi} \, d\xi \right] d\left(\frac{y}{S}\right) \qquad (5)$$

where ΔP_∞, $\Delta(C_p q)$ are the changes in pressure due to the Mach number gradient.

If we assume that the changes in Mach number are gradual over the chord of the wing so that $\Delta M = k(\xi - \frac{1}{2})$ and the flow is isentropic we get for first order changes in ΔM

$$\frac{\Delta P_\infty}{q} = \frac{-2}{M(1 + 0.2M^2)} \Delta M \qquad (6)$$

$$\frac{\Delta(C_p q)}{q} = C_p \frac{\Delta q}{q} + \Delta C_p \qquad (7)$$

$$\frac{\Delta \beta}{\beta} = \frac{M}{\beta^2} \Delta M \qquad (8)$$

$$\frac{\Delta q}{q} = \left(\frac{2}{M} - \frac{1.4M}{1 + 0.2M^2} \right) \Delta M \qquad (9)$$

The pressure coefficient (C_p) is dependent in a complicated way on the Mach number, but it is sufficiently accurate, for the arguments of this appendix, to assume it is inversely proportional to β. This gives

$$\Delta C_p = \frac{-C_p \Delta \beta}{\beta} \qquad (10)$$

so that on substituting in the integral for ΔC_{D_o} we get

$$\Delta C_{D_o} = 4 \int_o^1 \int_{y/S}^1 (A + BC_p)\left(\xi - \tfrac{1}{2}\right) \frac{\partial (Z/c_o)}{\partial \xi} \, d\xi \, d\left(\frac{y}{S}\right) \qquad (11)$$

where $A = \dfrac{-2k}{M(1 + 0.2M^2)}$, $\dfrac{B}{A} = \dfrac{0.6M^4}{\beta^2} - 1$ and $k = \dfrac{dM}{d\xi}$, the change in Mach number over the chord of the wing.

Since the ratio B/A is not large and C_p is small compared with unity the term BC_p has only a small effect on the integrand. Further since the size of the pressure is closely related to the local surface slope the influence of BC_p on the integrated result is very small. Hence we may take

$$\Delta C_{D_o} = 4 \int_o^1 \int_{y/S}^1 A\left(\xi - \tfrac{1}{2}\right) \frac{\partial (Z/c_o)}{\partial \xi} \, d\xi \, d\left(\frac{y}{S}\right) \qquad (12)$$

and on integrating by parts and reversing order of integration we get

$$\Delta C_{D_o} = -4A \int_o^1 \left\{ \int_o^\xi \frac{Z}{c_o} \, d\left(\frac{y}{S}\right) \right\} d\xi \qquad (13)$$

but

$$\frac{Z(\xi, y/S)}{c_o} = \frac{Z(\xi, 0)}{c_o}\left(1 - \frac{y}{S\xi}\right)$$

so that

$$\Delta C_{D_o} = -2A \int_o^1 \frac{Z(\xi, 0)}{c_o} \, \xi \, d\xi \qquad (14)$$

Appendix

The volume of the wing is given by the following equation

$$\frac{v}{c_o^3}\,\frac{c_o}{S} = 2\int_o^1 \frac{Z(\xi, 0)}{c_o}\,\xi\, d\zeta$$

so that the contribution to the drag coefficient is given by

$$\Delta C_{D_o} = \frac{2k\left(v/c_o^3\right)\left(c_o/S\right)}{M(1 + 0.2M^2)} \qquad (15)$$

where $k = \frac{dM}{d\xi}$, the change in Mach number over the chord of the wing.

It will be noted that equation (15) states that the buoyancy correction to drag is the product of the pressure gradient and the volume.

TABLE 1

Coefficients of wings

Ref. letter or number	Coefficients			
	A_0	A_1	A_2	A_3
1	22.38	6.38	-82.38	65.63
2	18.25	28.92	-123.58	90.42
3	14.00	52.67	-167.33	116.67
4	9.75	76.42	-211.08	142.92
E	33.30	-91.32	125.75	-58.83
G	31.95	-77.43	74.86	-12.04

TABLE 2

Reynolds numbers $\times 10^{-6}$ based on centre line chord for a non-laminar boundary layer at or very close to the disturbing elements

Mach number	Mean grain size (in.) / Re based on grain size	0.0018	0.0038	0.0051	0.0092
1.4	1200	8.0	3.8	2.8	1.6
1.58	1500	10.0	4.7	3.5	2.0
2.01	2000	13.3	6.3	4.7	2.6
2.19	2300	15.3	7.2	5.4	3.0

Printed in England for Her Majesty's Stationery Office by the Royal Aircraft Establishment, Farnborough. R.T.58.K.4.

TABLE 3

Summary of results

Wing	Mach No.	$\frac{\beta S}{c_o}$	$\frac{S'(1)}{c_o} / \frac{v}{c_o^3}$	$S''(1) / \frac{v}{c_o^3}$	$S''(0) / \frac{v}{c_o^3}$	K_o thin-wing theory	K_o slender body theory	K_o experiment		ΔK_o	
								Re 4×10^6	Re 8×10^6	Re 4×10^6	Re 8×10^6
3	1.40	0.245	-16.0	-200.0	28.0	1.090	0.641	0.920	0.976	-0.170	-0.114
E	1.40	0.245	- 8.9	- 31.4	66.6	0.952	1.000	0.925	0.930	-0.027	-0.022
3	1.58	0.306	-16.0	-200.0	28.0	1.021	0.413	0.990	0.995	-0.031	-0.026
E	1.58	0.306	- 8.9	- 31.4	66.6	0.879	0.933	0.875	0.895	-0.004	0.016
1	2.01	0.436	-12.0	-125.0	44.75	0.830	0.360	0.771	0.771	-0.059	-0.059
2	2.01	0.436	-14.0	-162.0	36.5	0.867	0.213	0.777	0.791	-0.090	-0.076
3	2.01	0.436	-16.0	-200.0	28.0	0.915	0.068	0.824	0.834	-0.091	-0.081
4	2.01	0.436	-18.0	-238.0	19.5	0.975	-0.103	0.898	0.915	-0.077	-0.060
E	2.01	0.436	- 8.9	- 31.4	66.6	0.755	0.825	0.739	0.744	-0.016	-0.011
G	2.01	0.436	-17.34	- 34.68	63.9	0.908	0.550	0.788	0.791	-0.120	-0.117
								Re 4×10^6	Re 7×10^6	Re 4×10^6	Re 7×10^5
3	2.19	0.487	-16.0	-200.0	28.0	0.889	-0.049	0.834	0.849	-0.055	-0.040
E	2.19	0.487	- 8.9	- 31.4	66.6	0.720	0.795	0.729	0.729	+0.009	+0.009

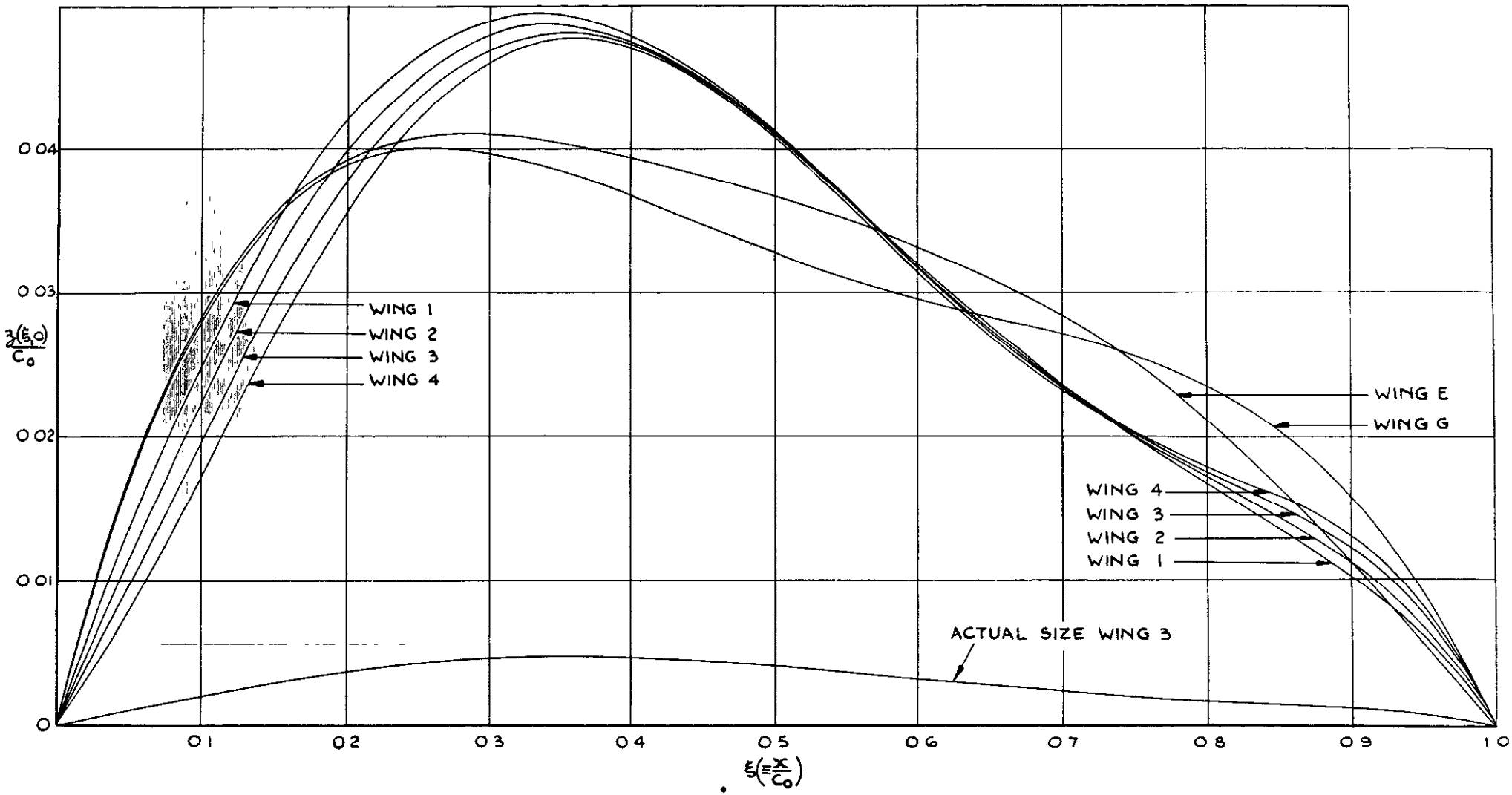

FIG. 1. NON - DIMENSIONAL CENTRE LINE THICKNESS DISTRIBUTION - ALL WINGS

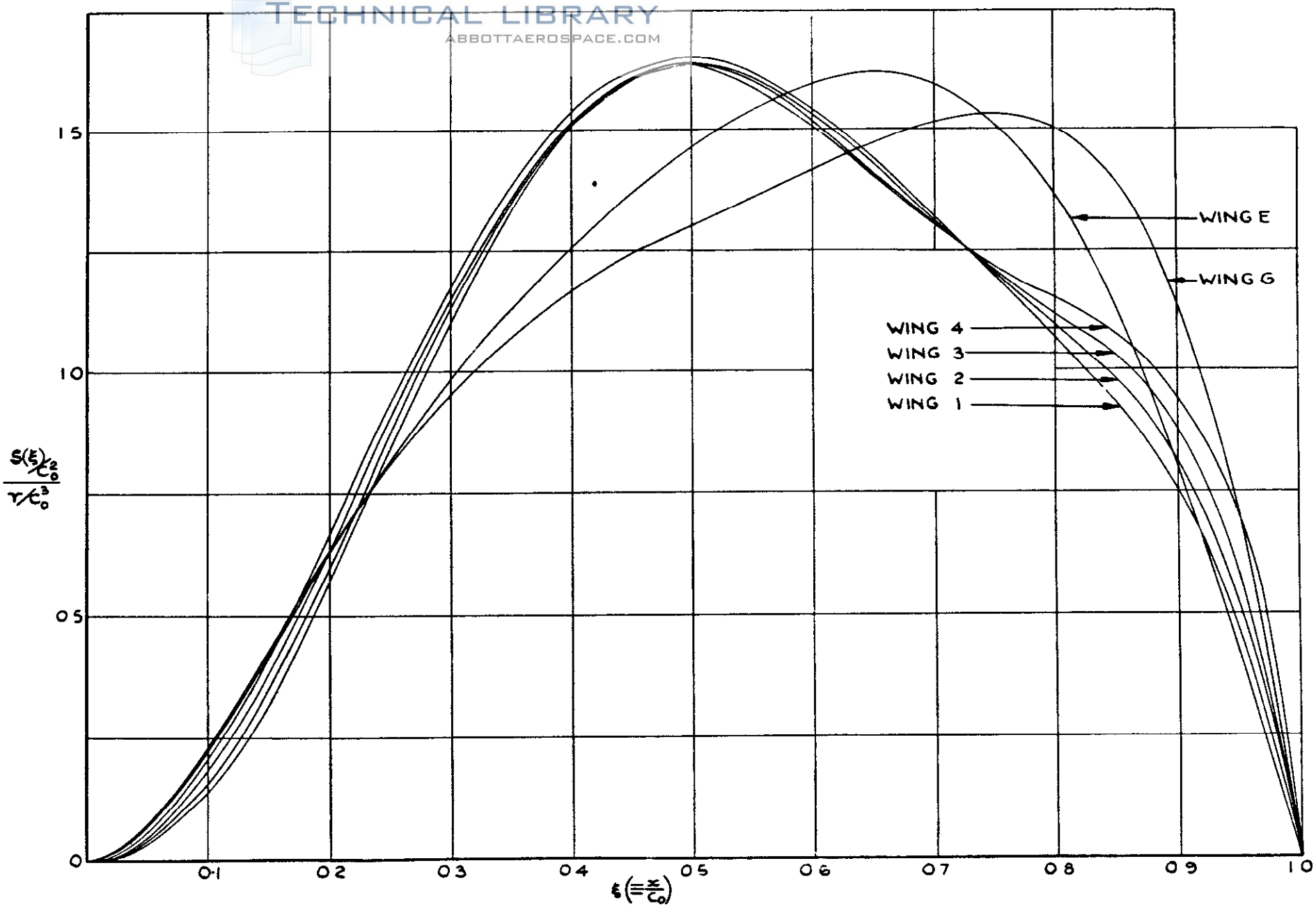

FIG. 2. NON-DIMENSIONAL AREA DISTRIBUTIONS - ALL WINGS.

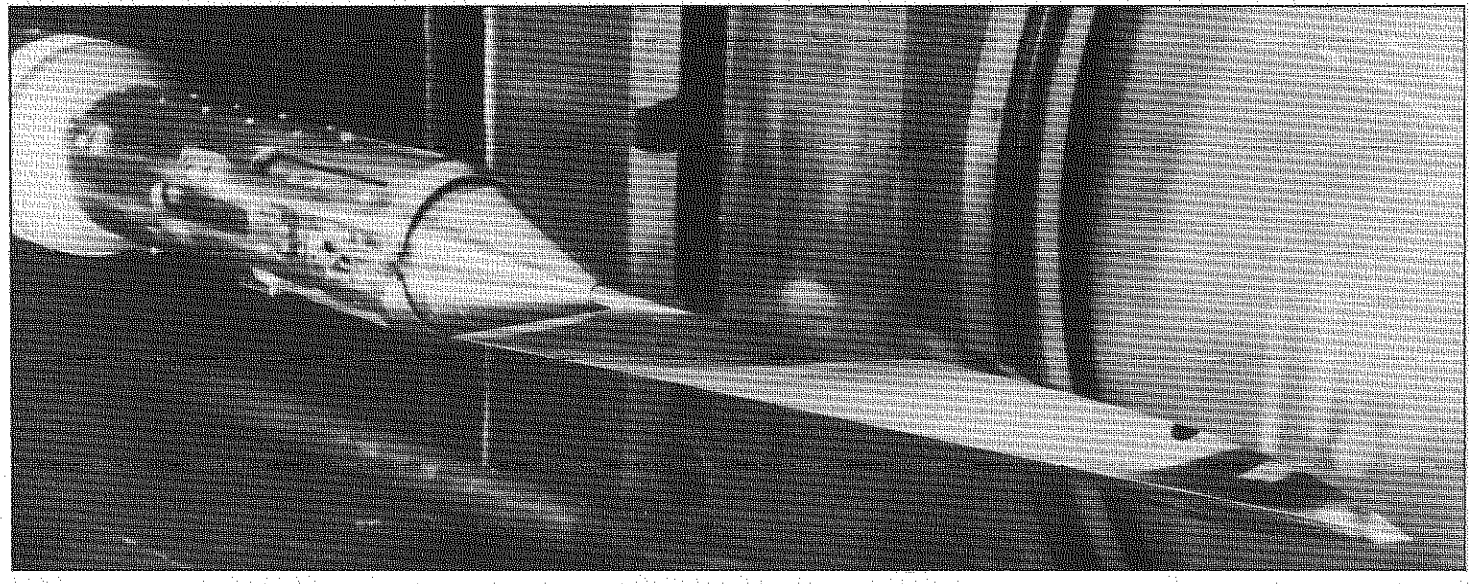

a. SUPPORT TUBE RETRACTED

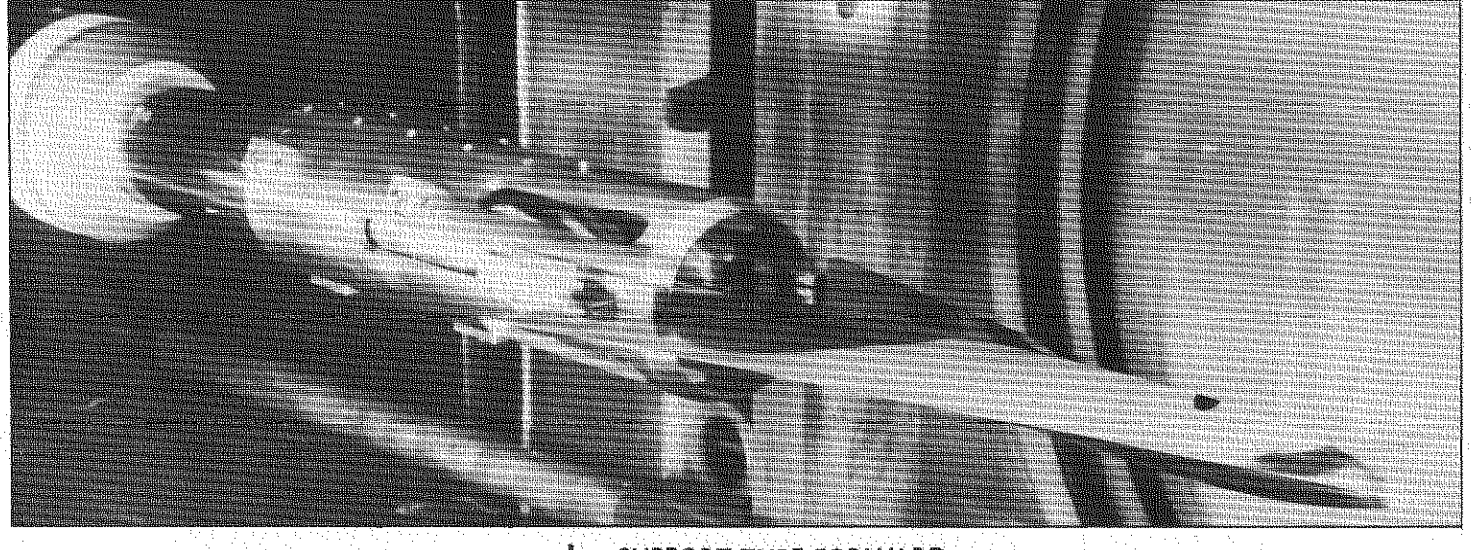

b. SUPPORT TUBE FORWARD

FIG.3. WING E, MOUNTED IN No.19 (18"x18") SUPERSONIC WIND TUNNEL

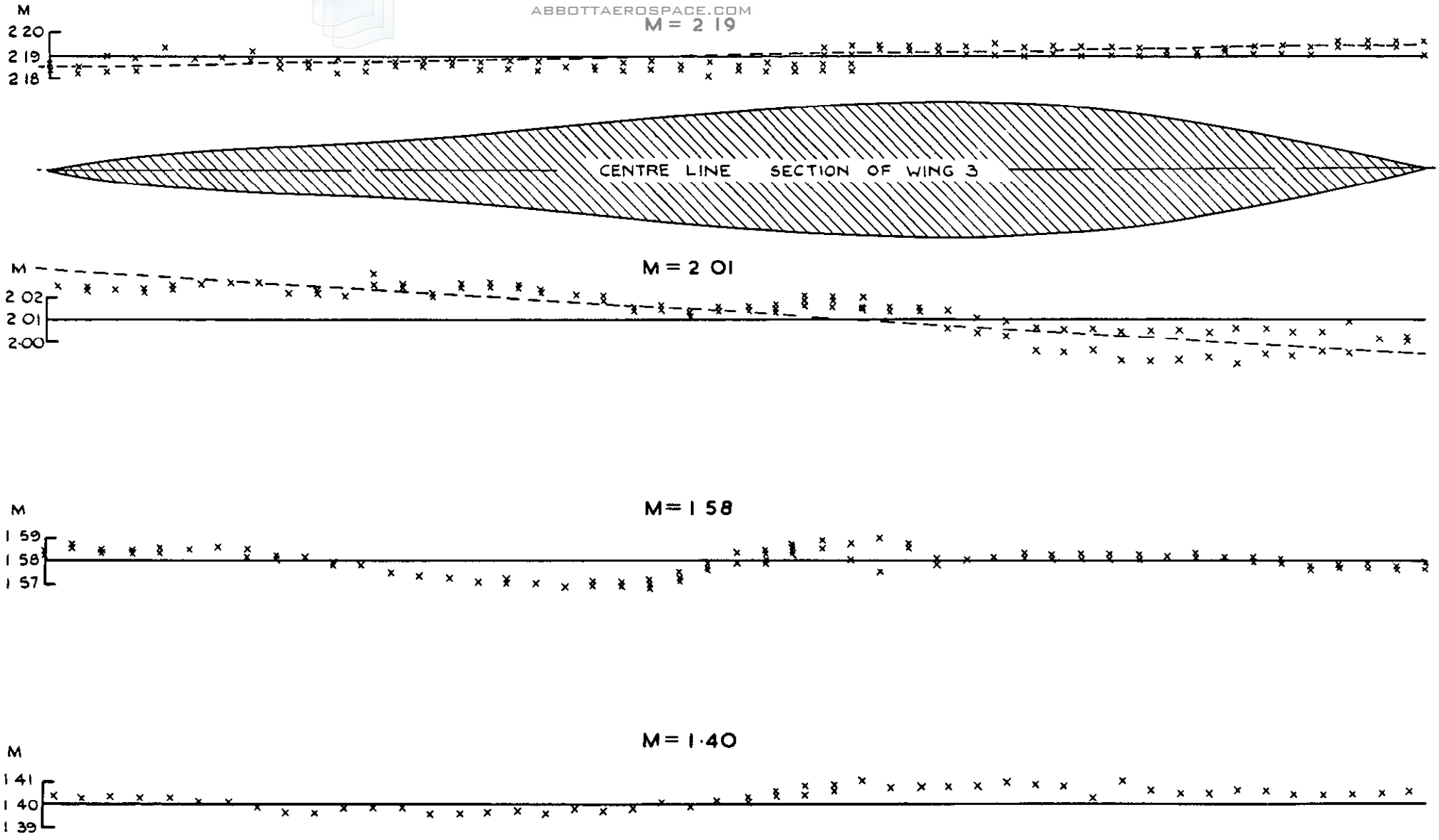

FIG. 4. CENTRE LINE MACH NUMBER DISTRIBUTION IN No. 19 (18" X 18") TUNNEL.

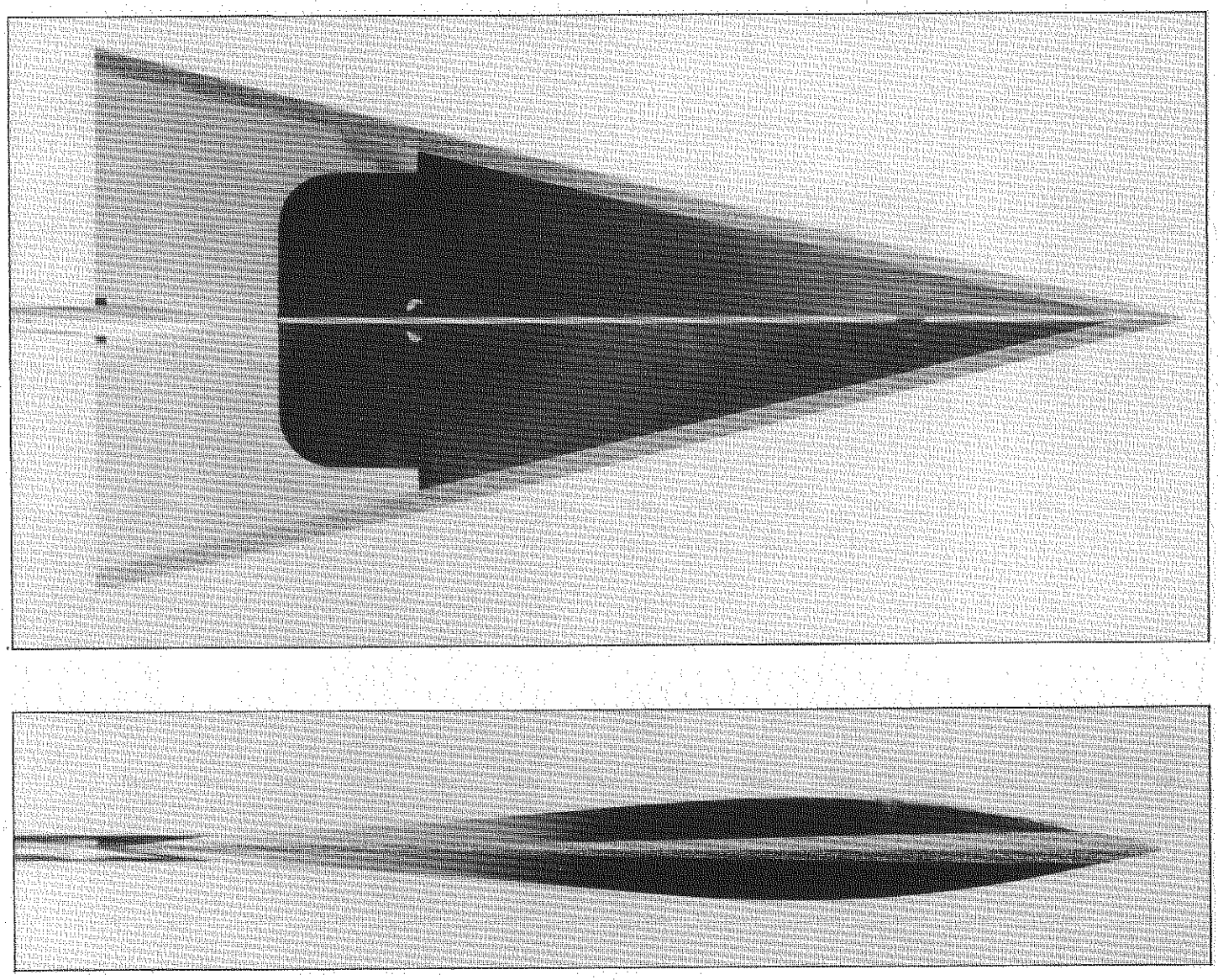

FIG.5. MODEL 2 WITH 0·0038 in. GRAIN SIZE TRANSITION BANDS

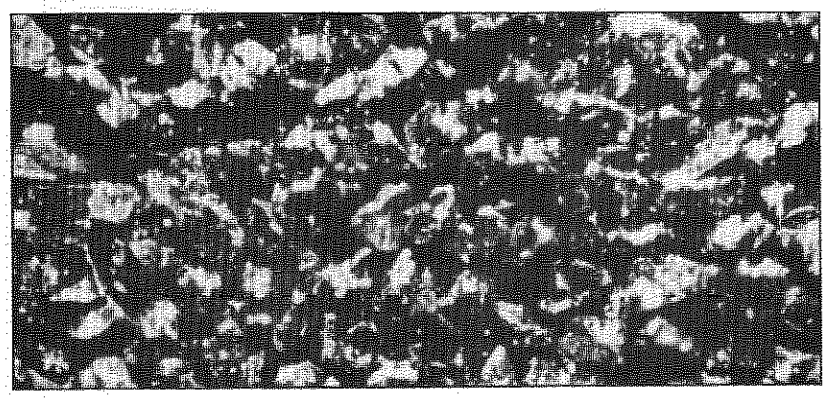

0·0092 inches

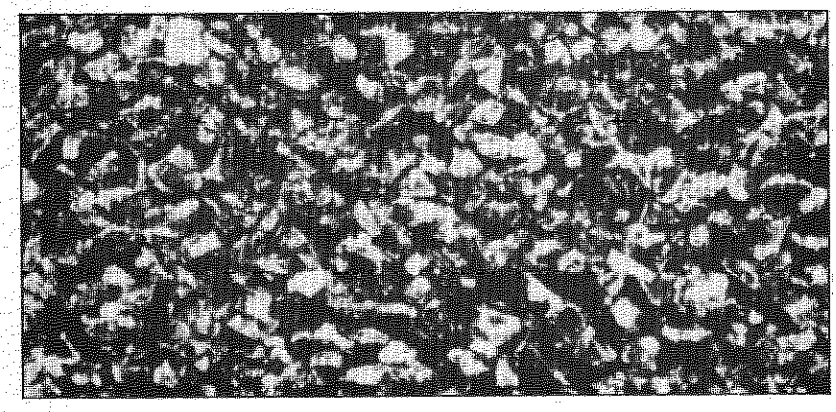

0·0051 inches

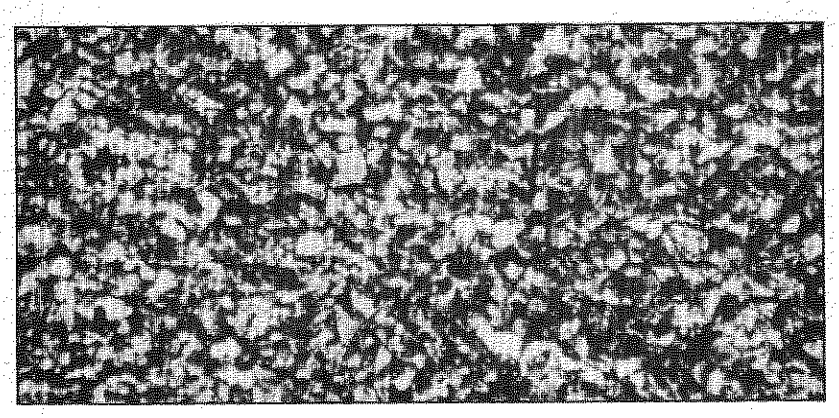

0·0038 inches

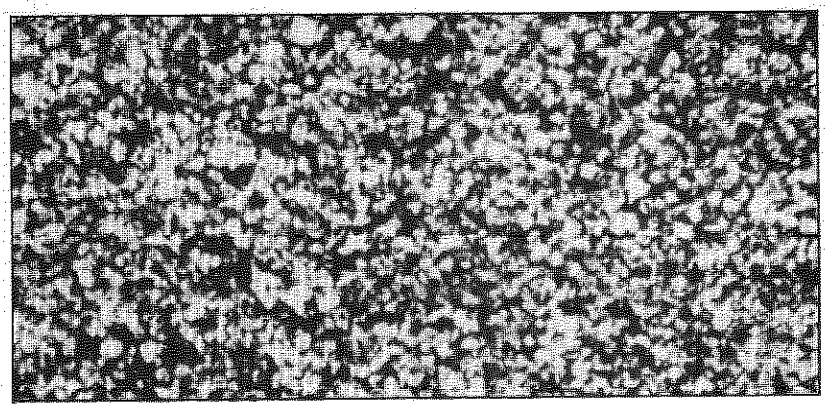

0·0018 inches

FIG.6. PHOTOMICROGRAPHS (x25) OF TRANSITION BANDS MEAN GRAIN SIZES GIVEN

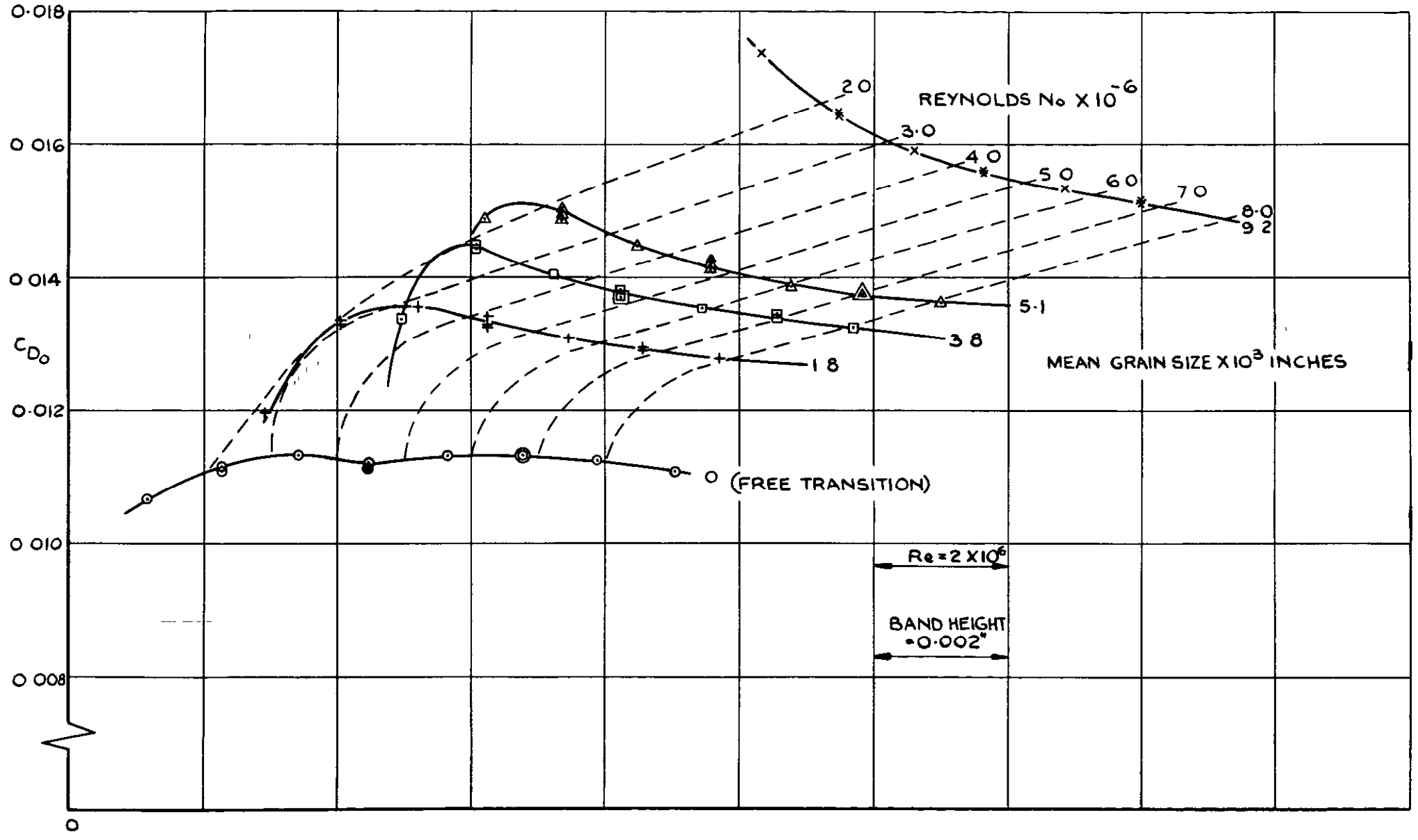

FIG. 7(a) MEASURED DRAG AT ZERO LIFT - WING 3 - M = 1·40

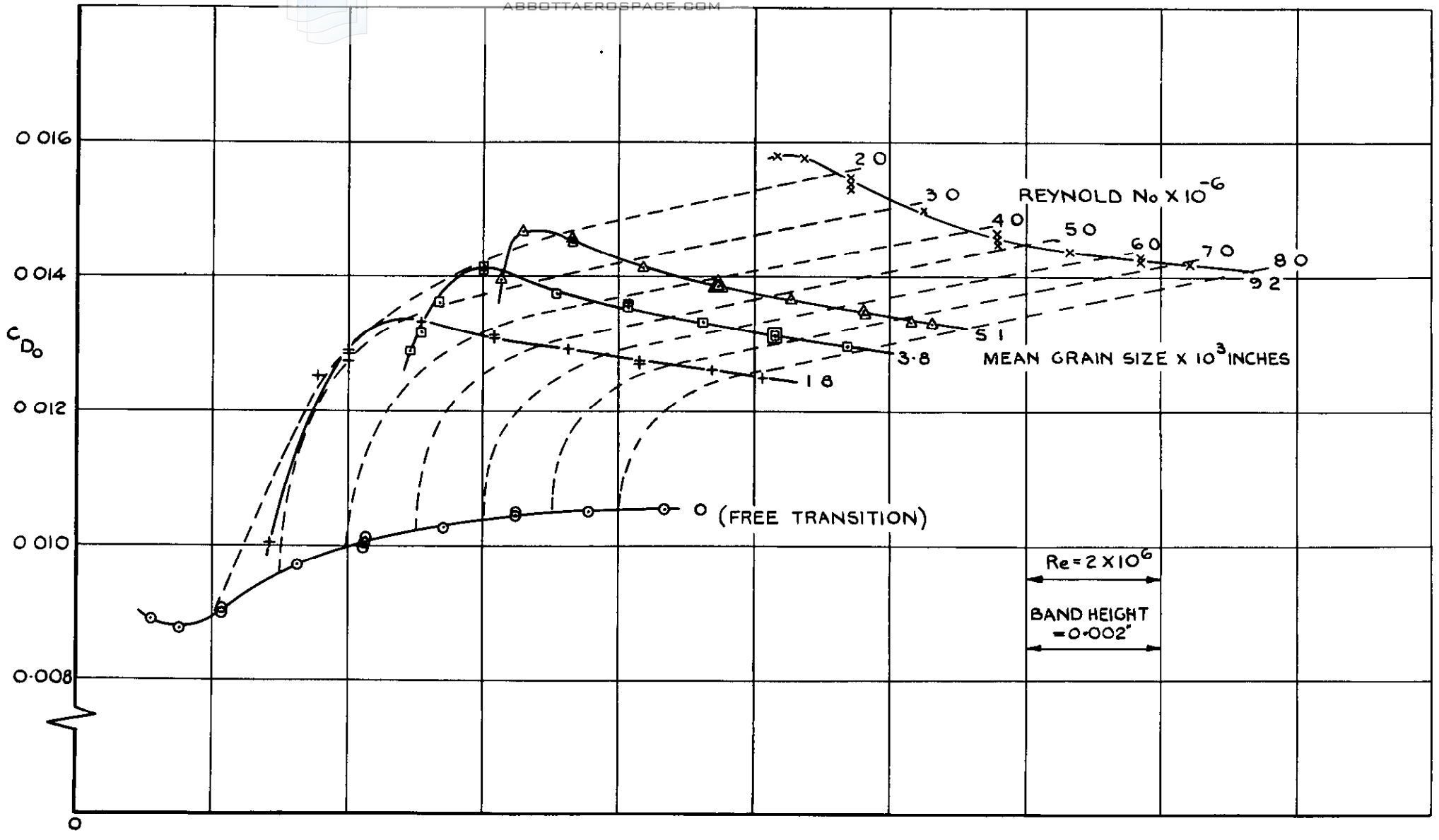

FIG. 7 (b) MEASURED DRAG AT ZERO LIFT - WING 3 - M = 1.58

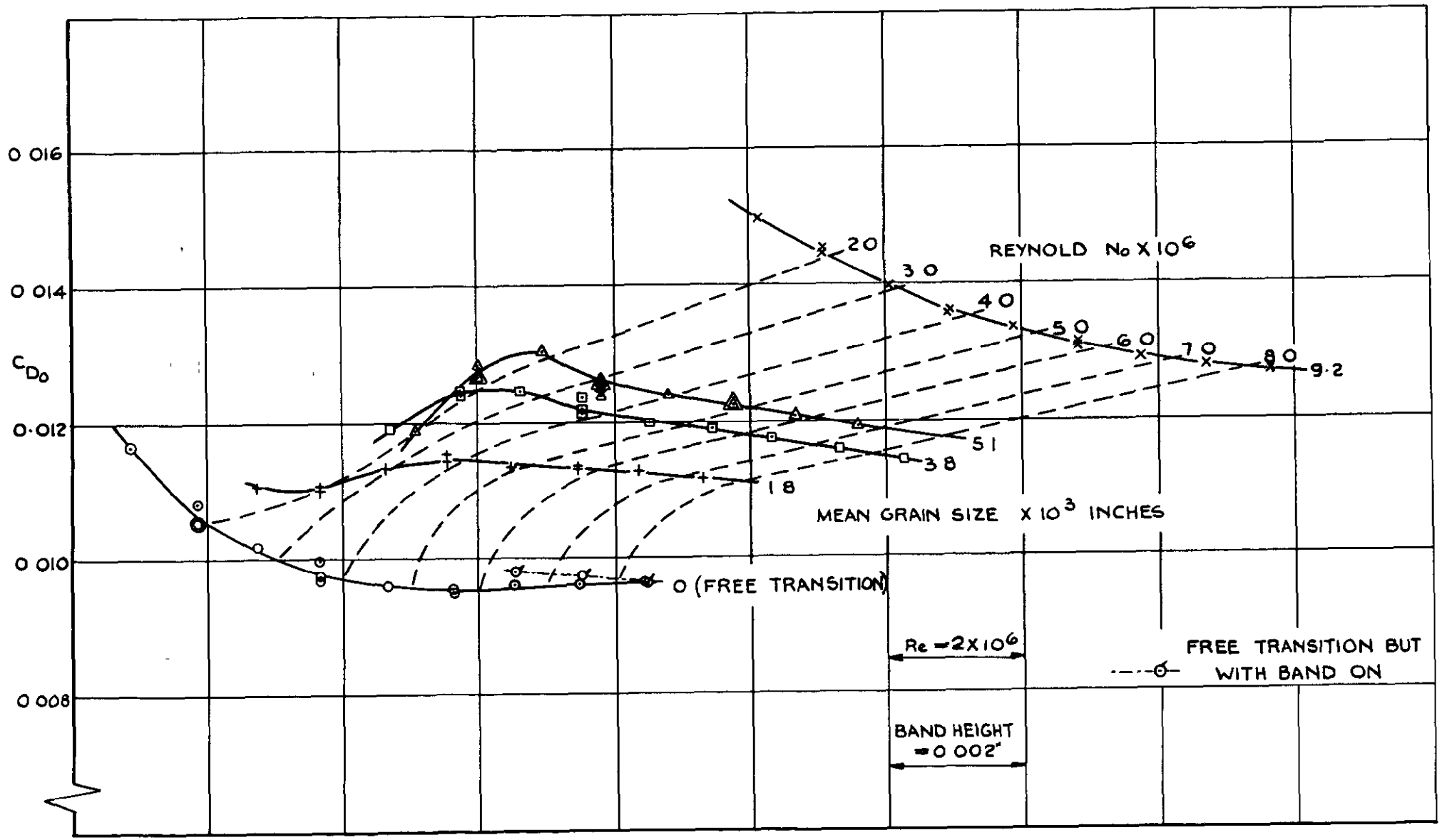

FIG. 7(c) MEASURED DRAG AT ZERO LIFT - WING 3 – M = 2·01

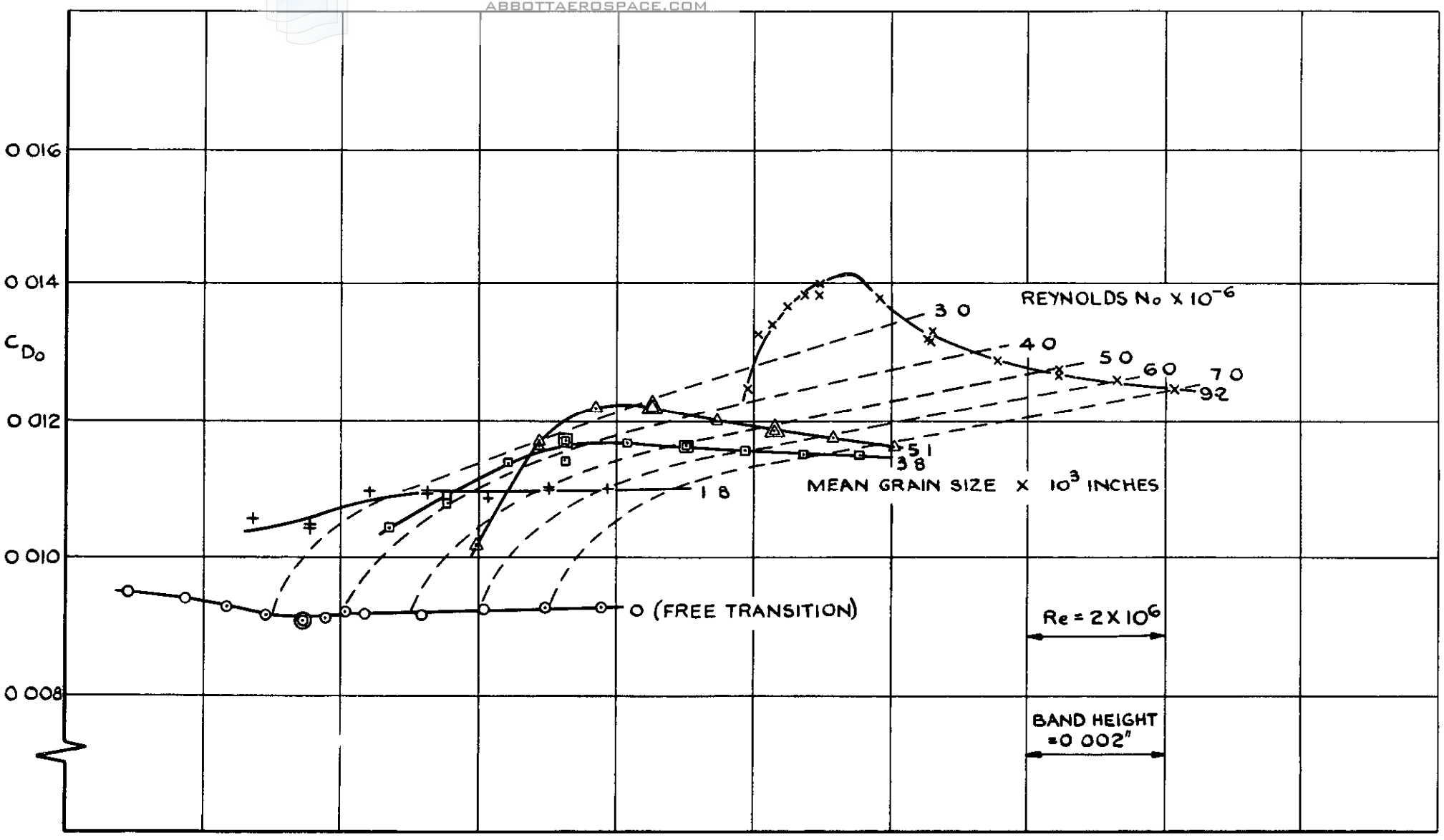

FIG. 7 (d) MEASURED DRAG AT ZERO LIFT - WING 3 M = 2·19

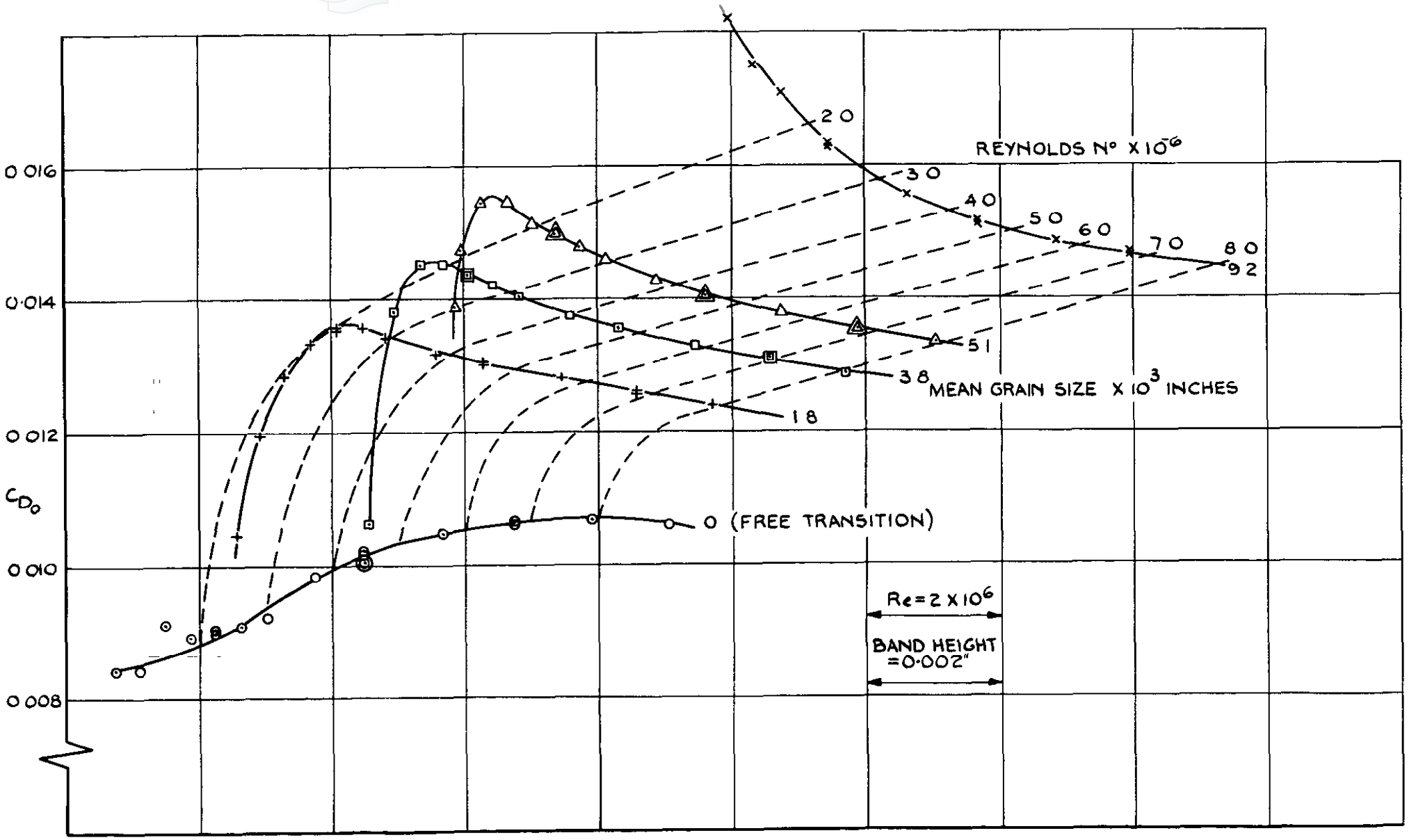

FIG. 8(a) MEASURED DRAG AT ZERO LIFT - WING E - M = 1·40

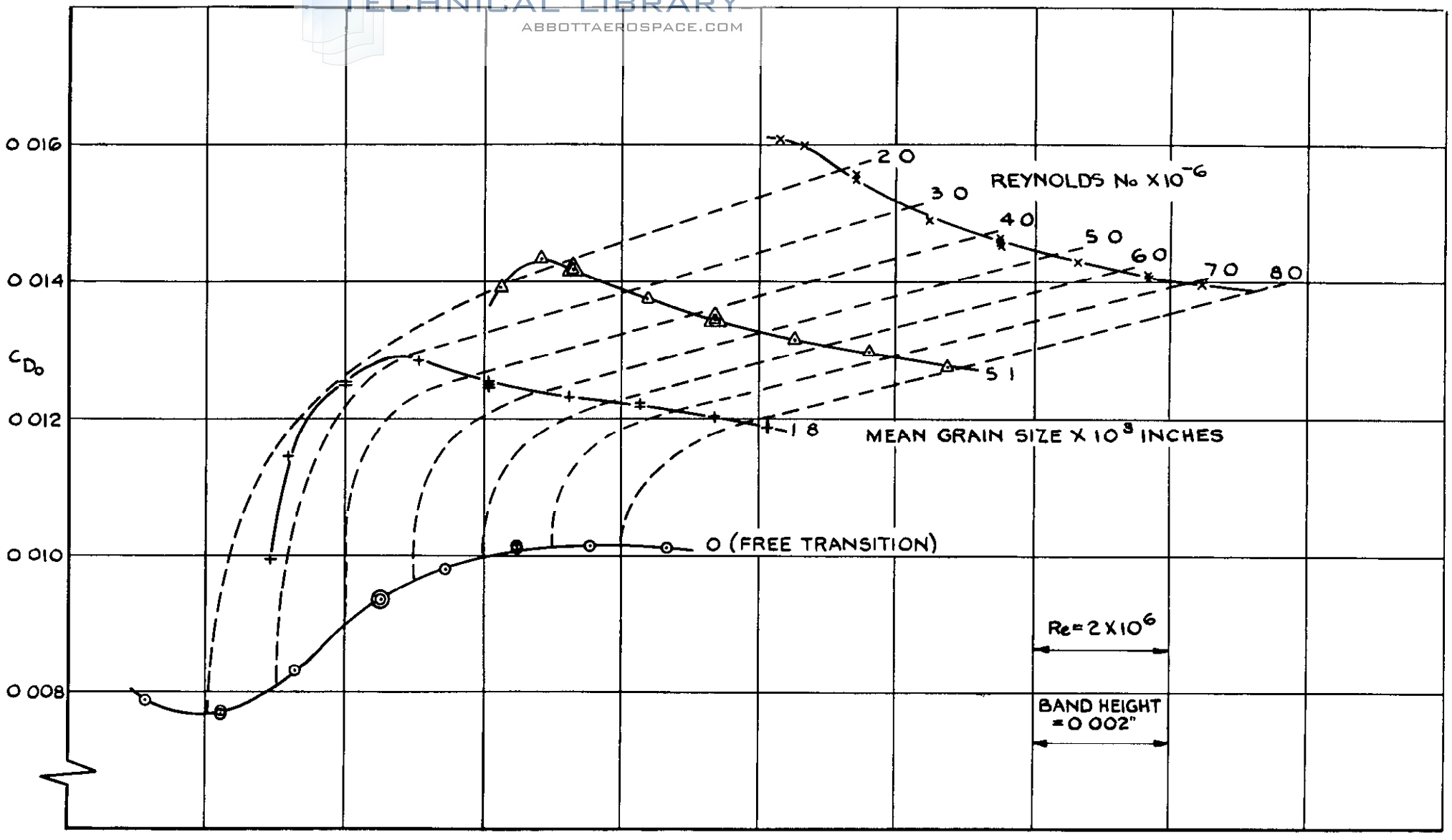

FIG. 8 (b) MEASURED DRAG AT ZERO LIFT - WING E M=1·58

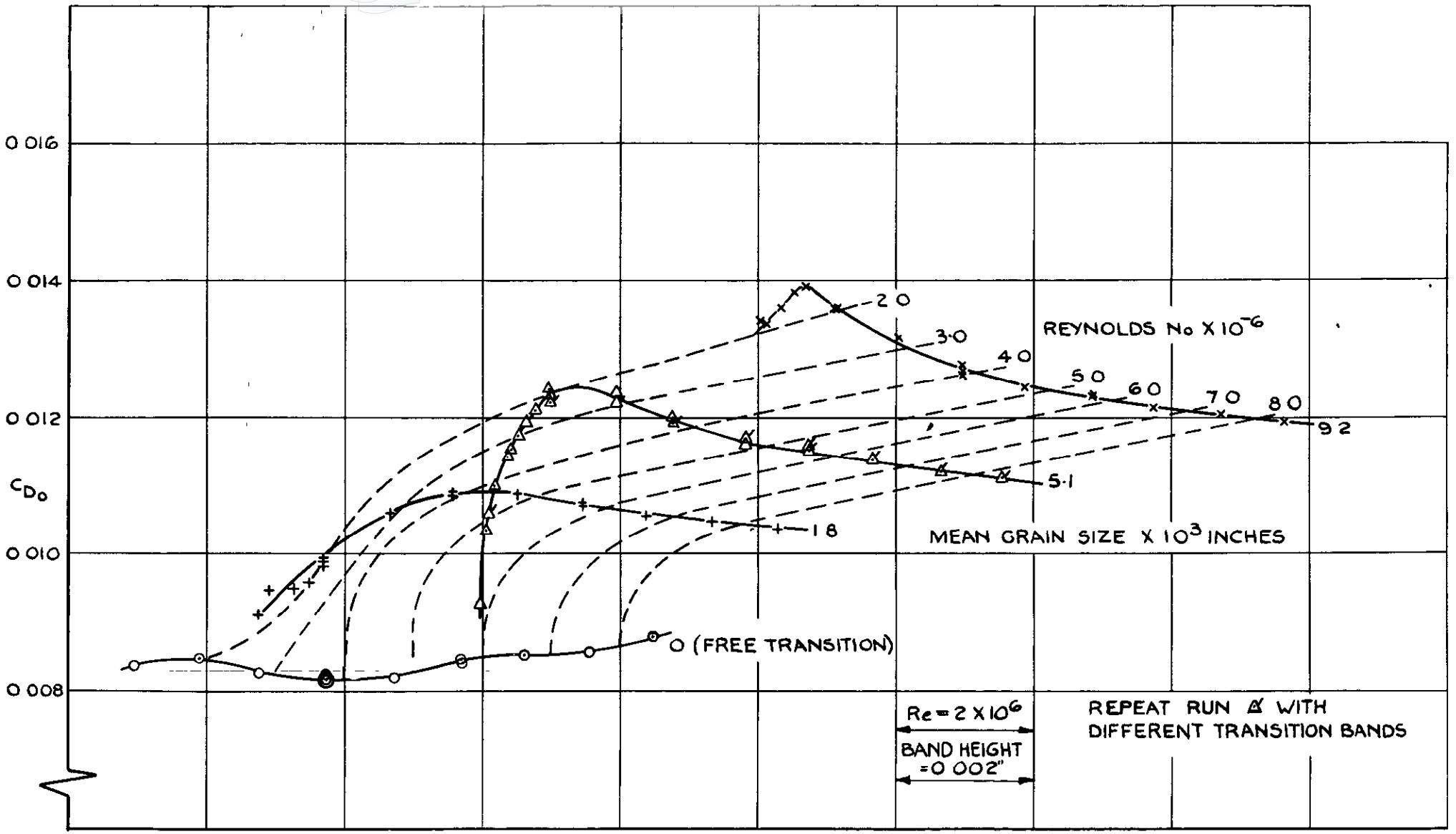

FIG. 8(c) MEASURED DRAG AT ZERO LIFT - WING E M= 2·01

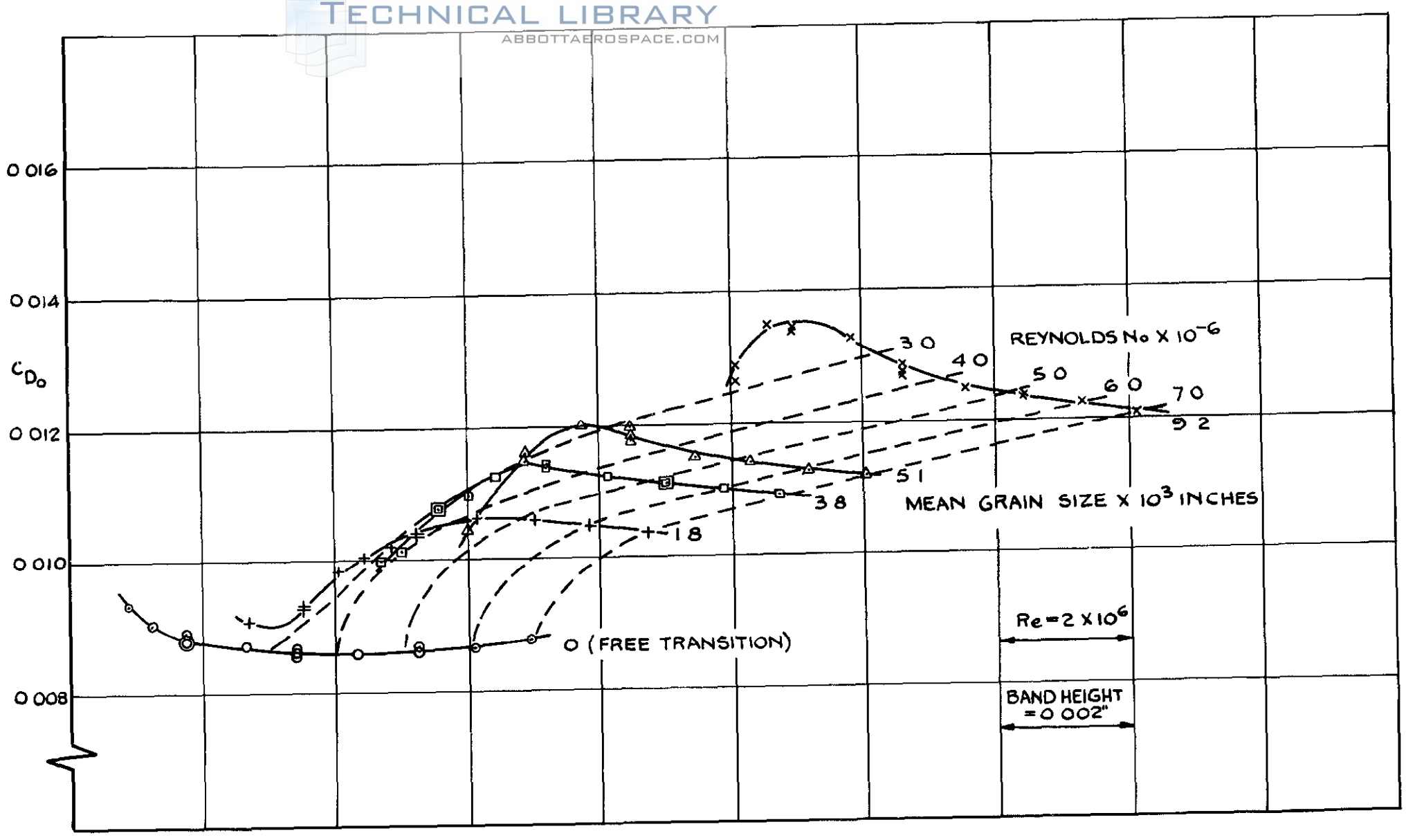

FIG. 8 (d) MEASURED DRAG AT ZERO LIFT – WING E M = 2·19

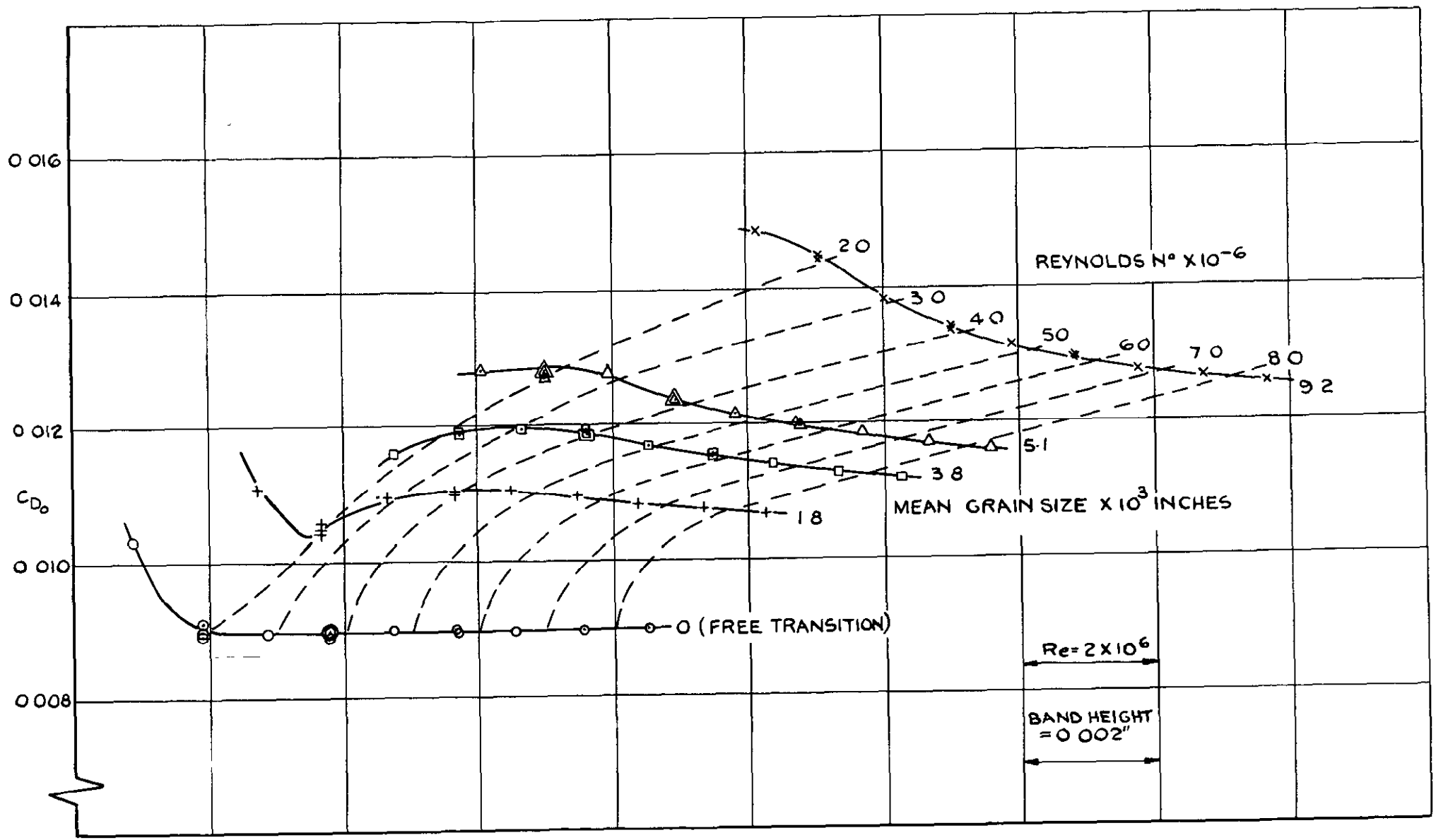

FIG. 9 (a) MEASURED DRAG AT ZERO LIFT - WING 1 - M = 2·01

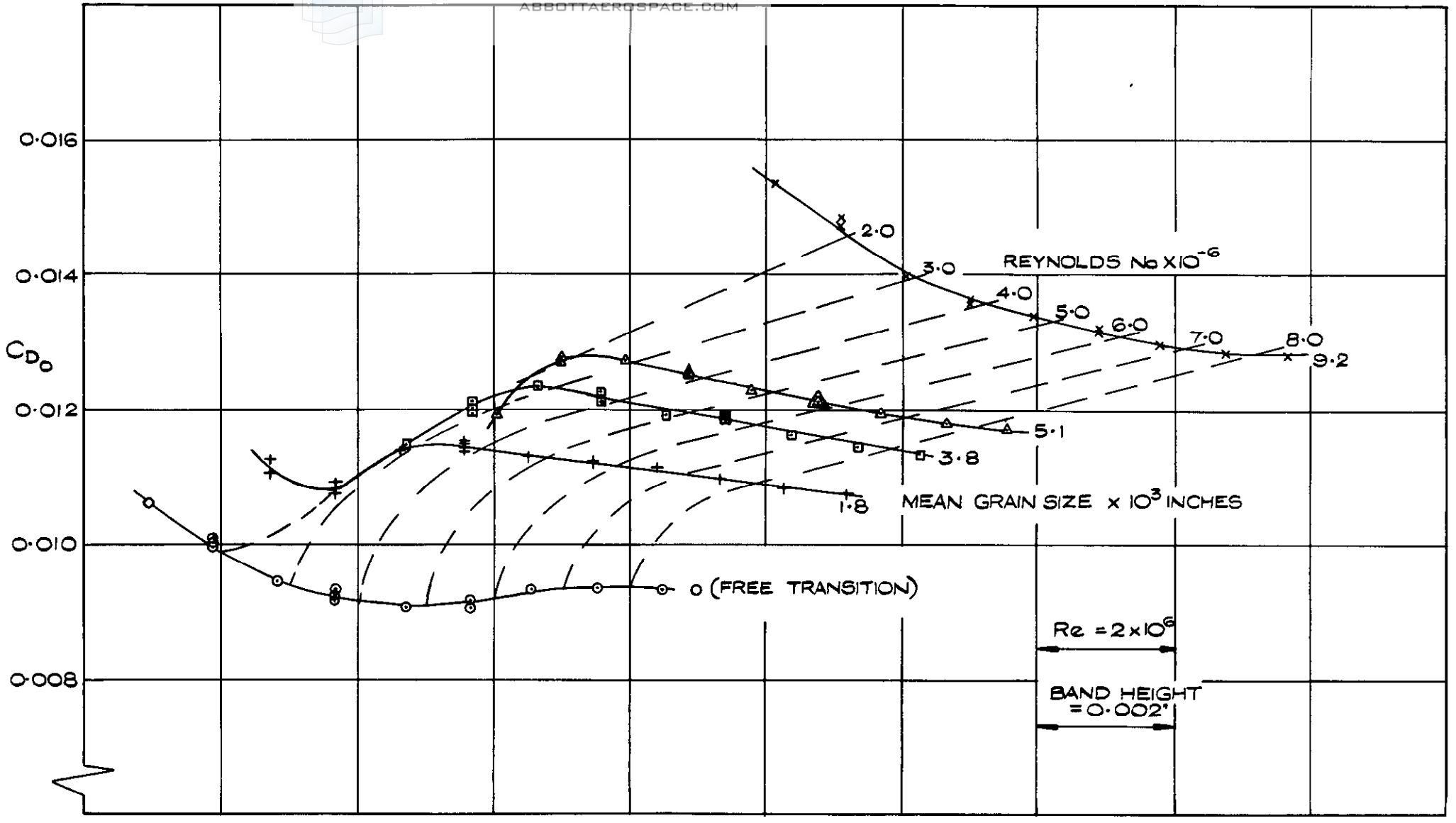

FIG. 9 (b) MEASURED DRAG AT ZERO LIFT – WING 2 – M = 2·01

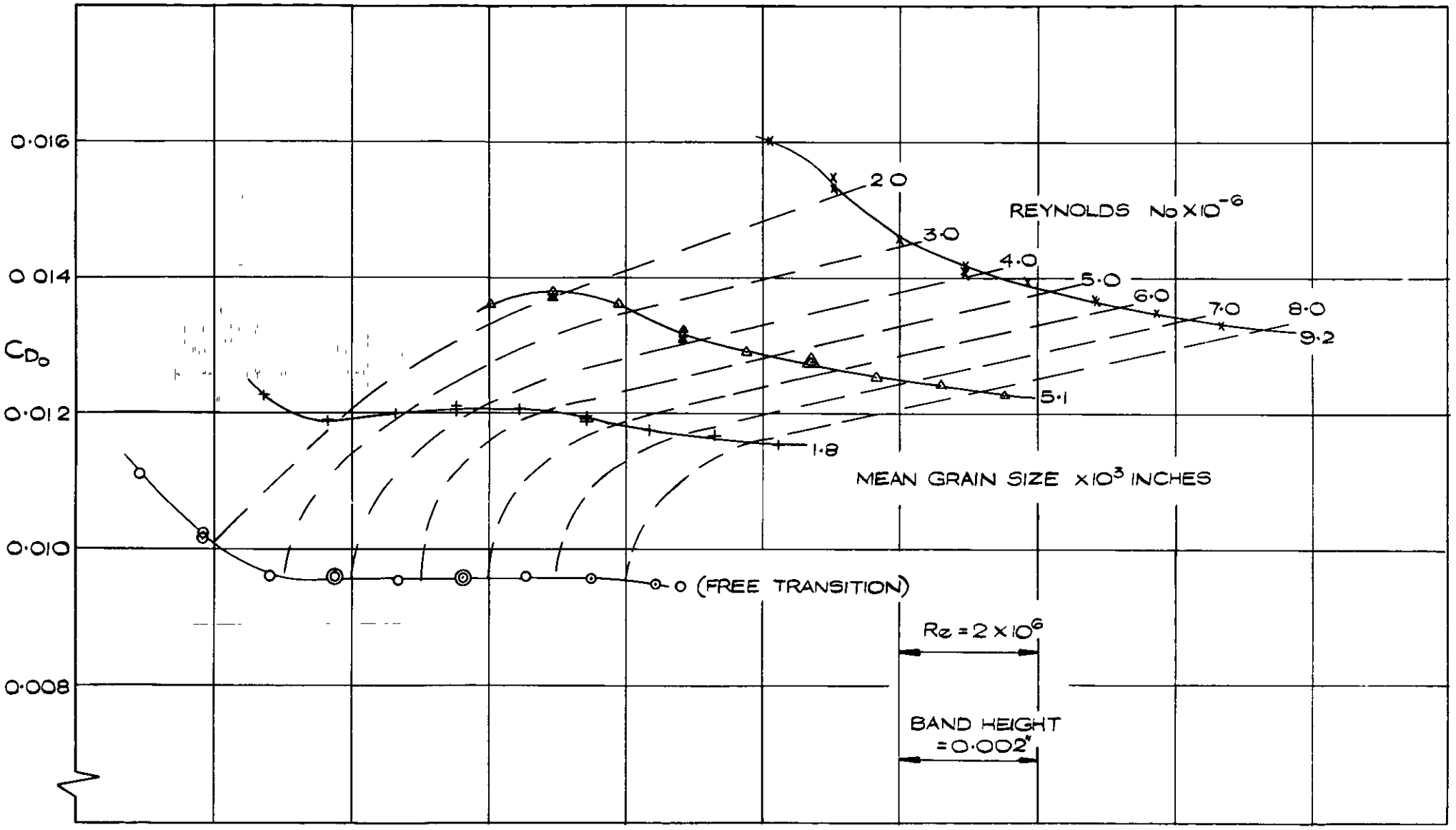

FIG 9(c) MEASURED DRAG AT ZERO LIFT - WING 4 - M = 2·01

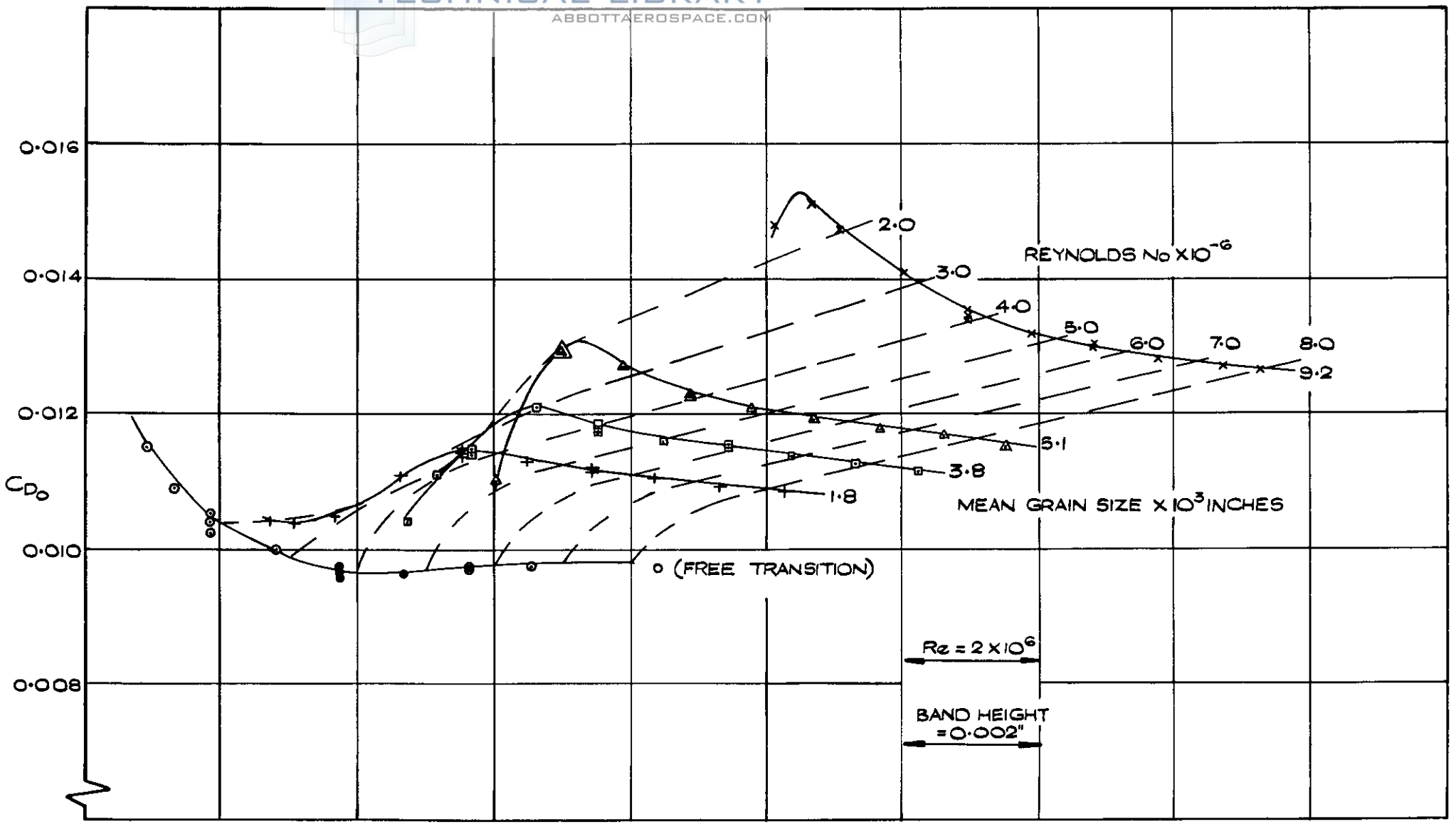

FIG. 9(d) MEASURED DRAG AT ZERO LIFT - WING. G. - M = 2·01

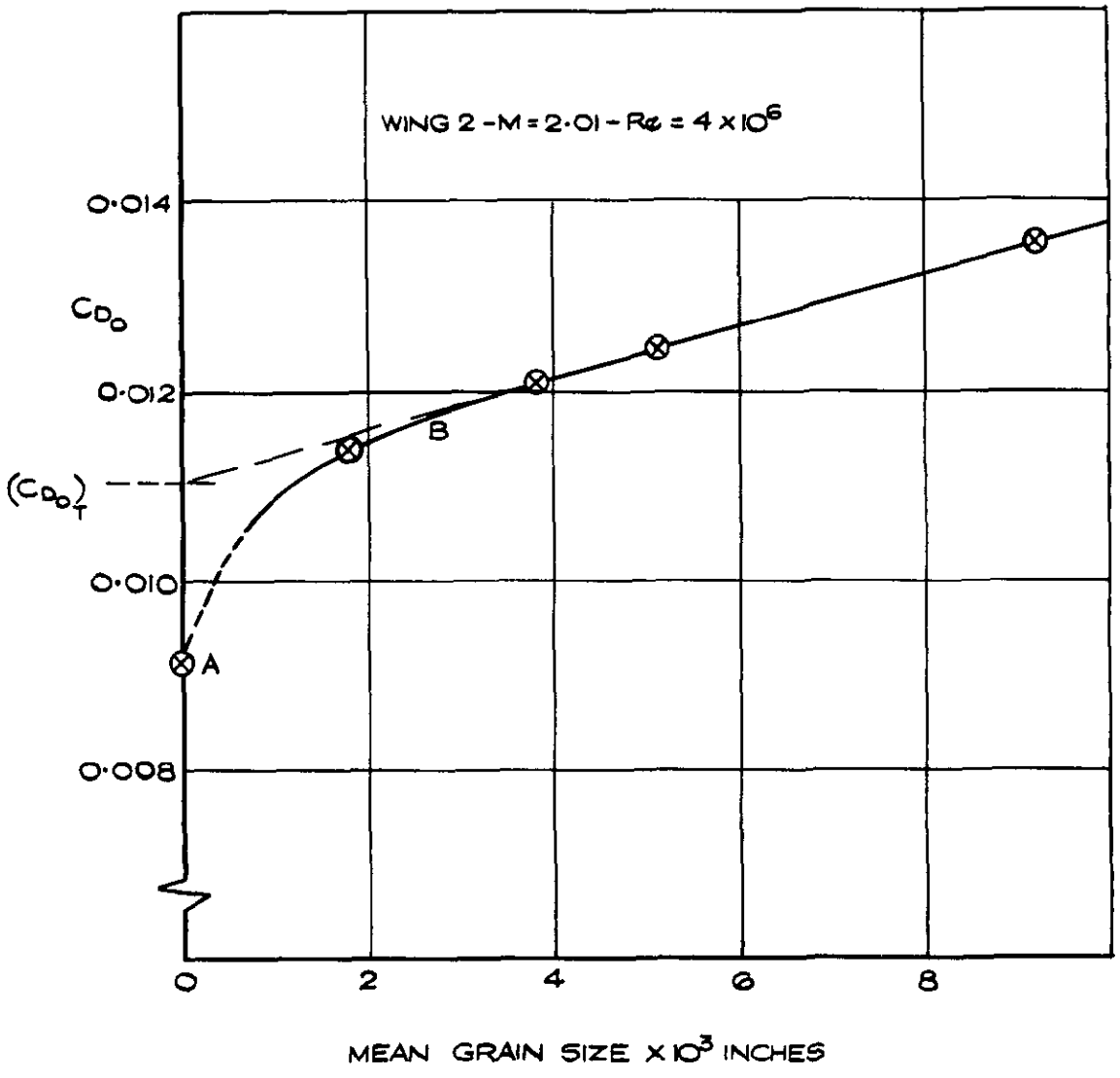

FIG. 10. DETERMINATION OF C_{D_o} FOR WING WITH A FULLY TURBULENT BOUNDARY LAYER $[(C_{D_o})_T]$

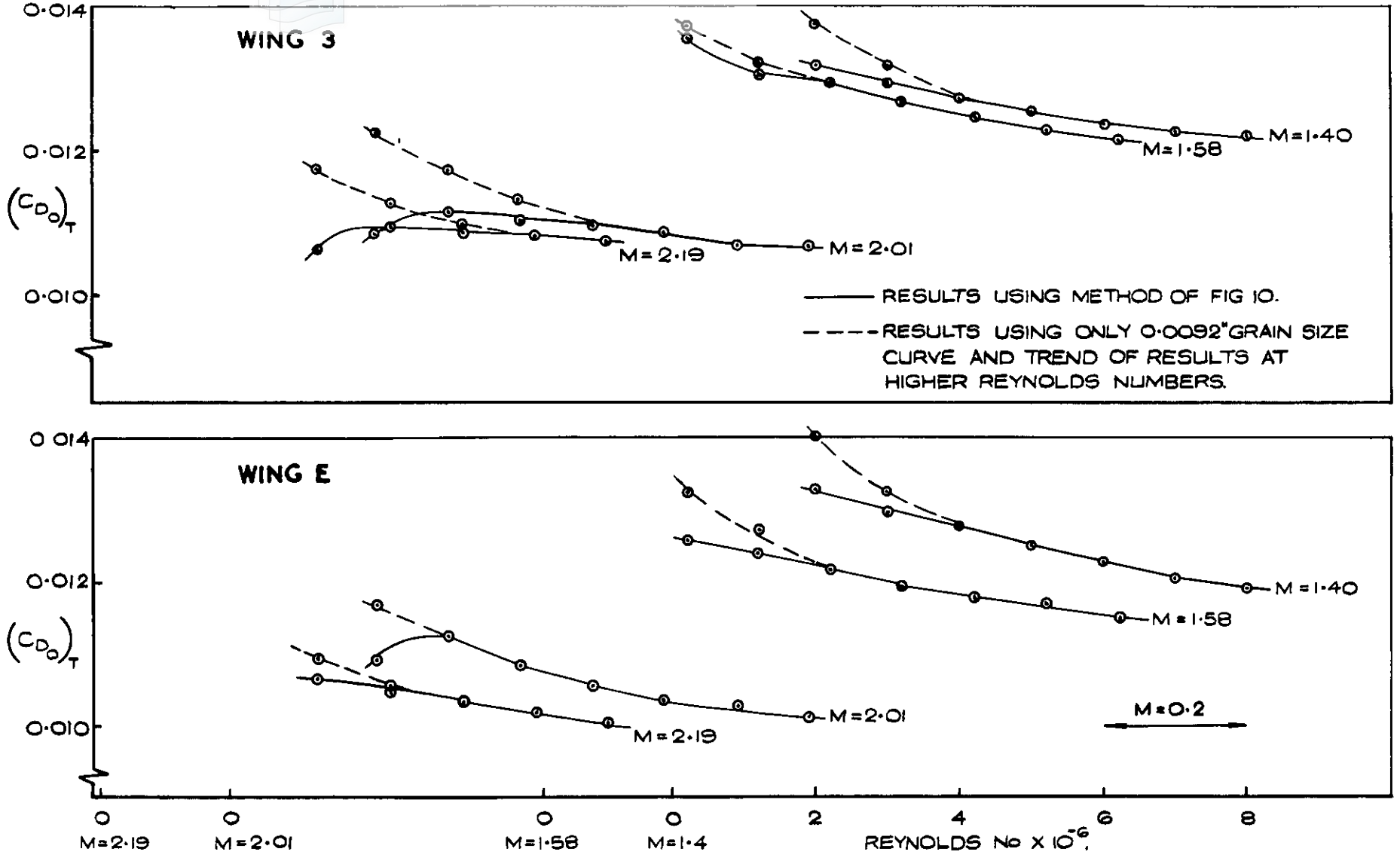

FIG. 11. $(C_{D_0})_T$ FOR WING 3. AND WING E.

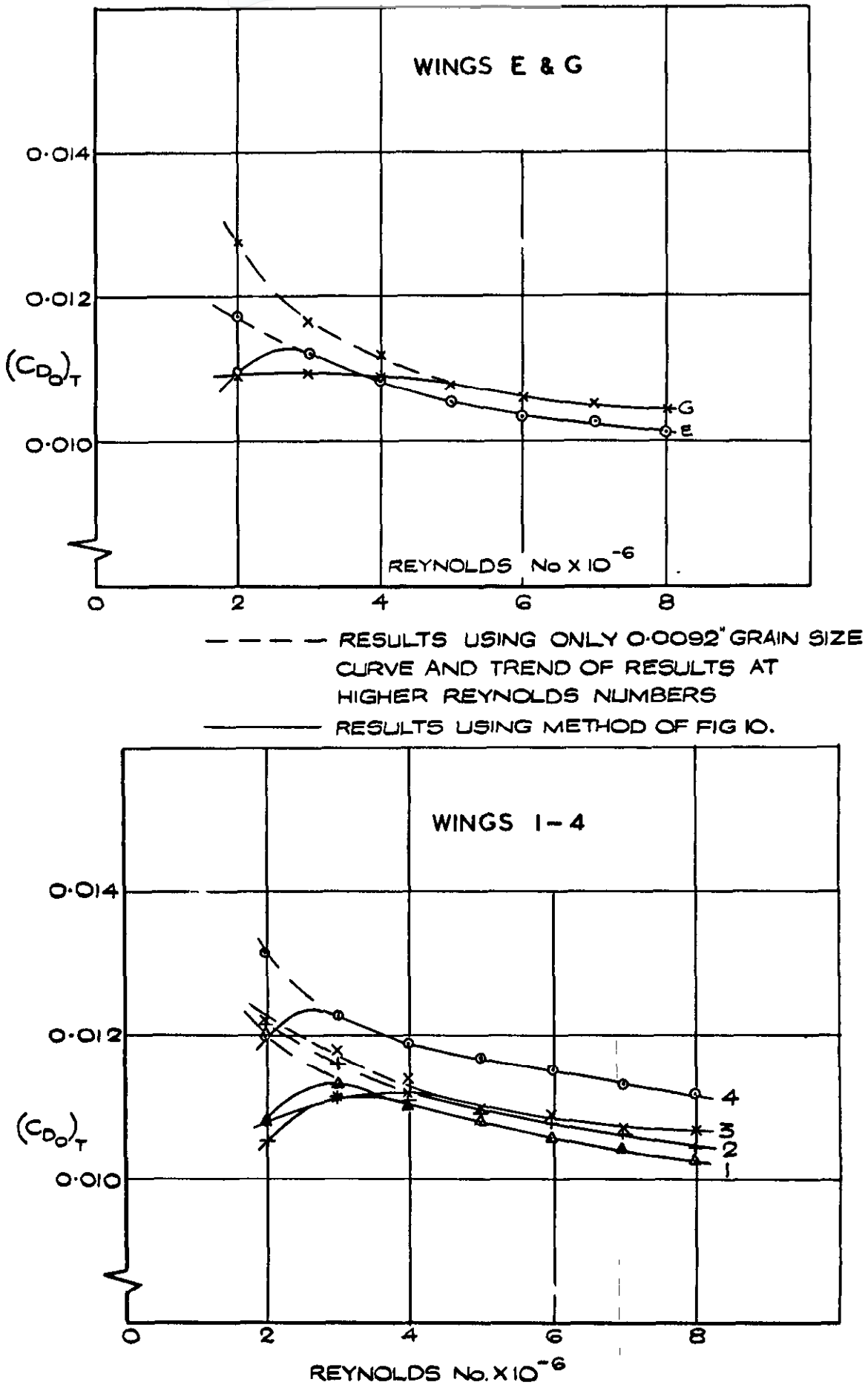

— — — — RESULTS USING ONLY 0·0092" GRAIN SIZE CURVE AND TREND OF RESULTS AT HIGHER REYNOLDS NUMBERS

———— RESULTS USING METHOD OF FIG 10.

FIG.12. $(C_{D_o})_T$ FOR WINGS TESTED AT M = 2·01.

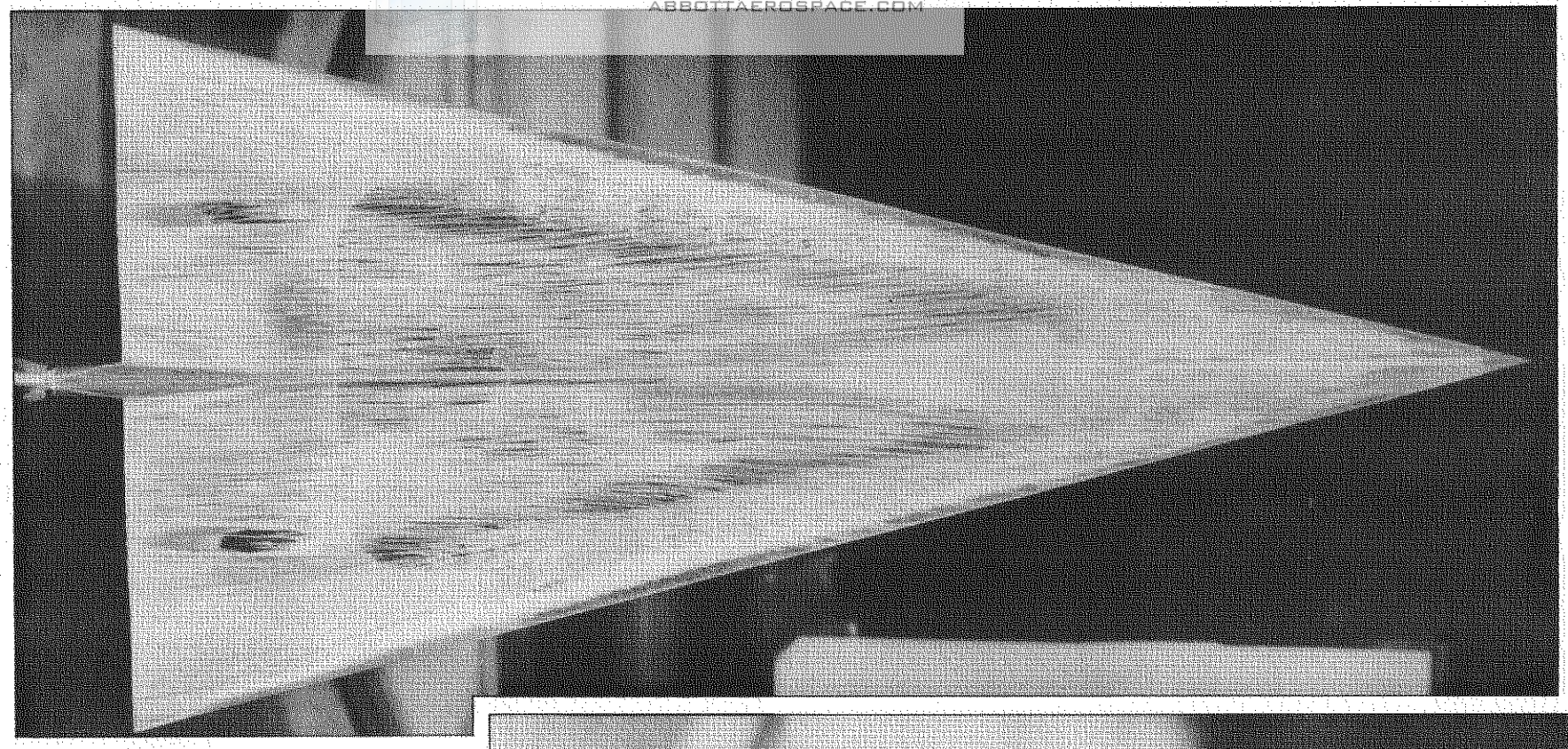

$R_e = 3 \cdot 75 \times 10^6$

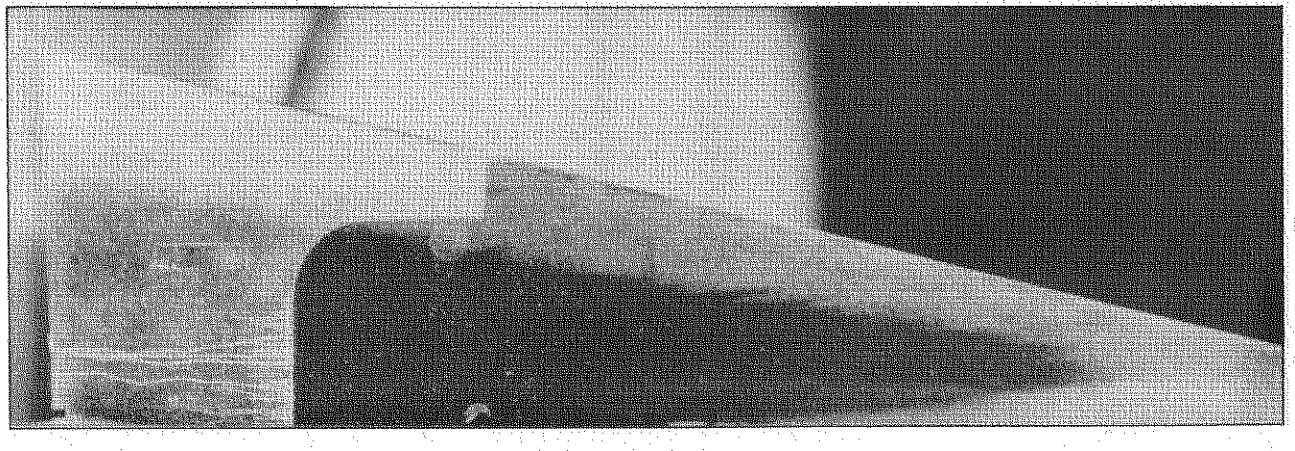

FIG.13. OIL FLOW ON WING 2, INDICATING TRANSITION AS A CHANGE IN OIL FLOW PATTERN WITH CONFIRMATION FROM AZOBENZENE SUBLIMATION

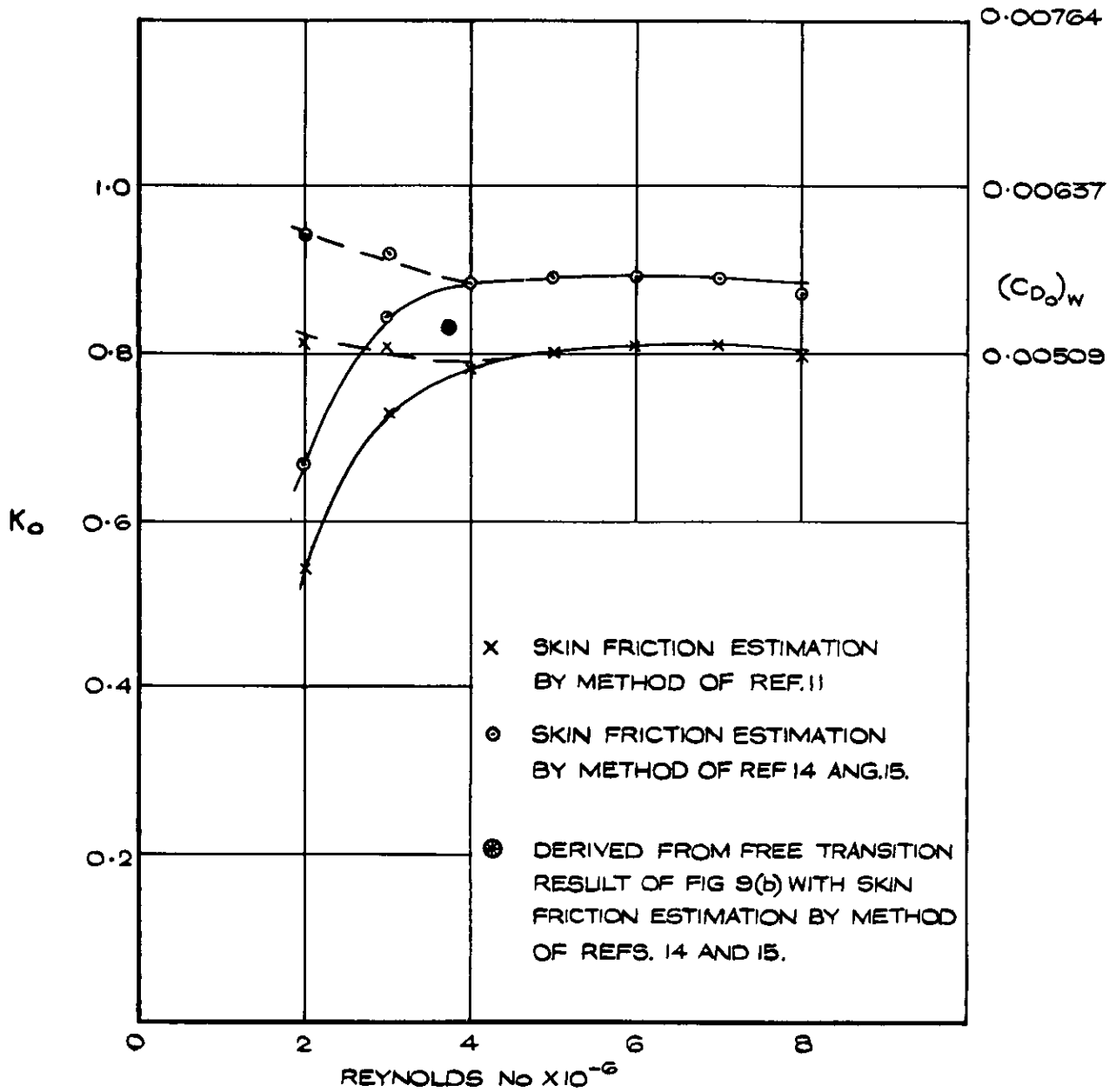

FIG. 14. DERIVED WAVE DRAG FACTORS (K_o)
M = 2·01 – WING 2.

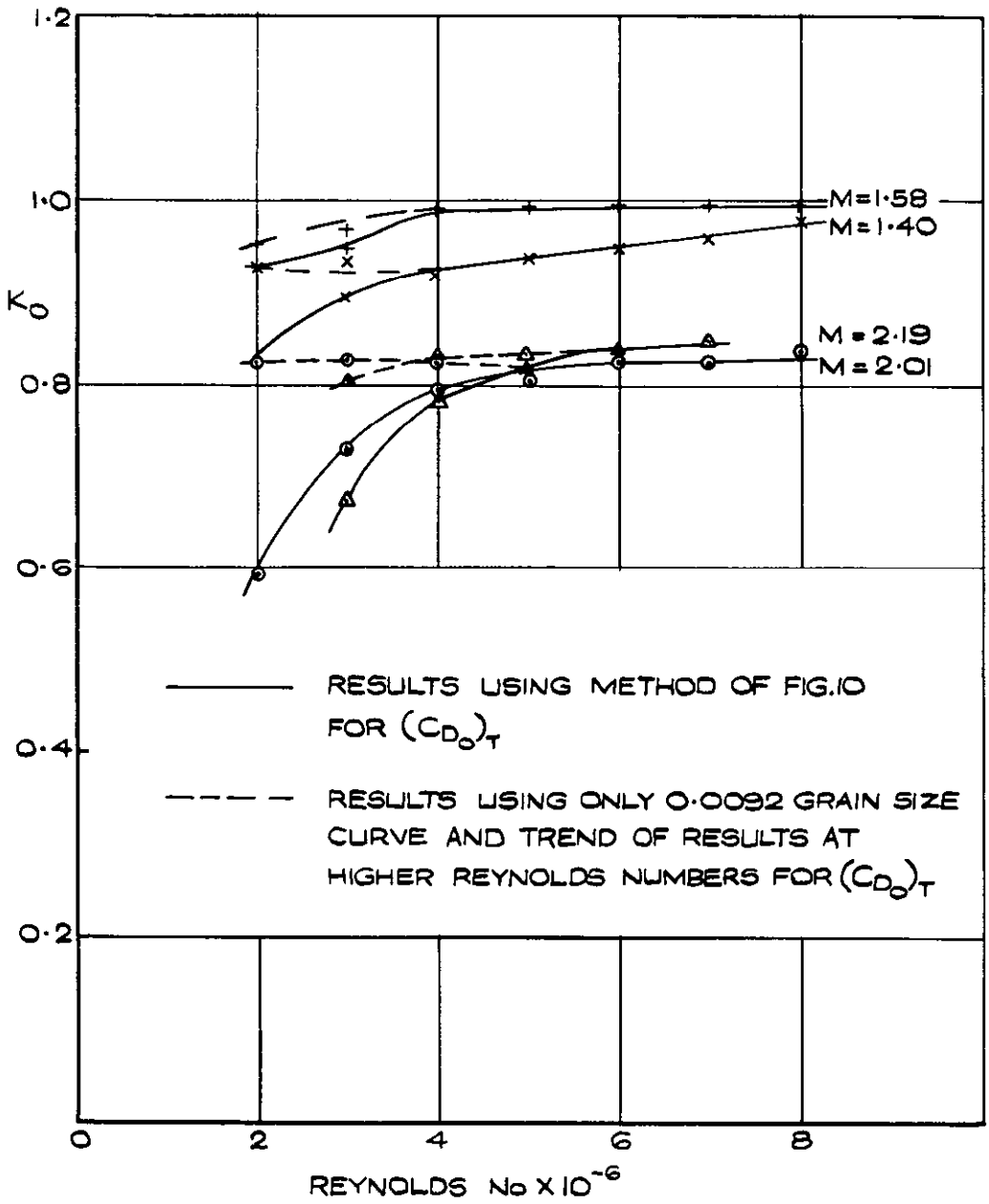

FIG. 15. DERIVED WAVE DRAG FACTORS (K_o) WING 3.

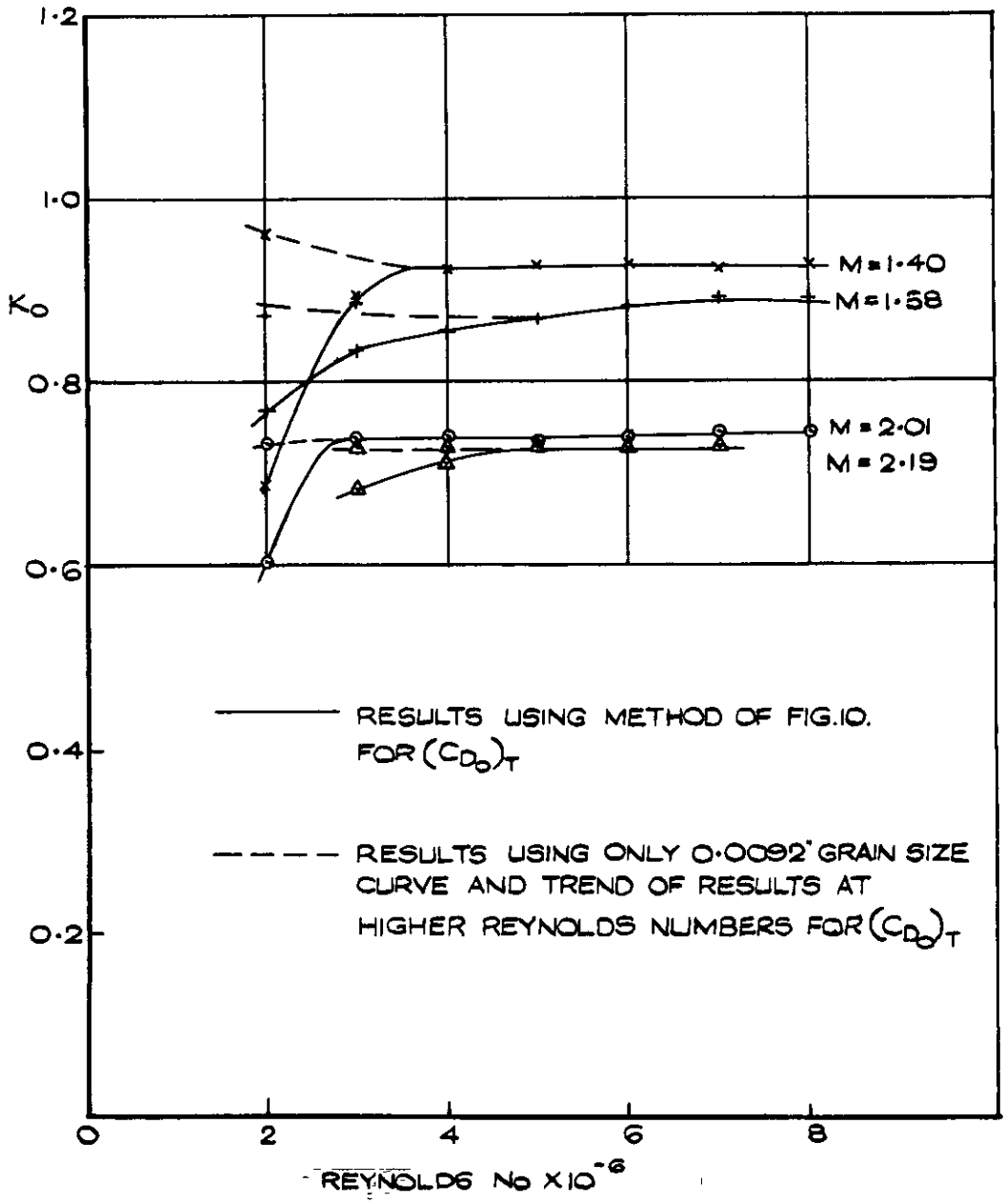

FIG.16. DERIVED WAVE DRAG FACTORS (K_o) -WING E.

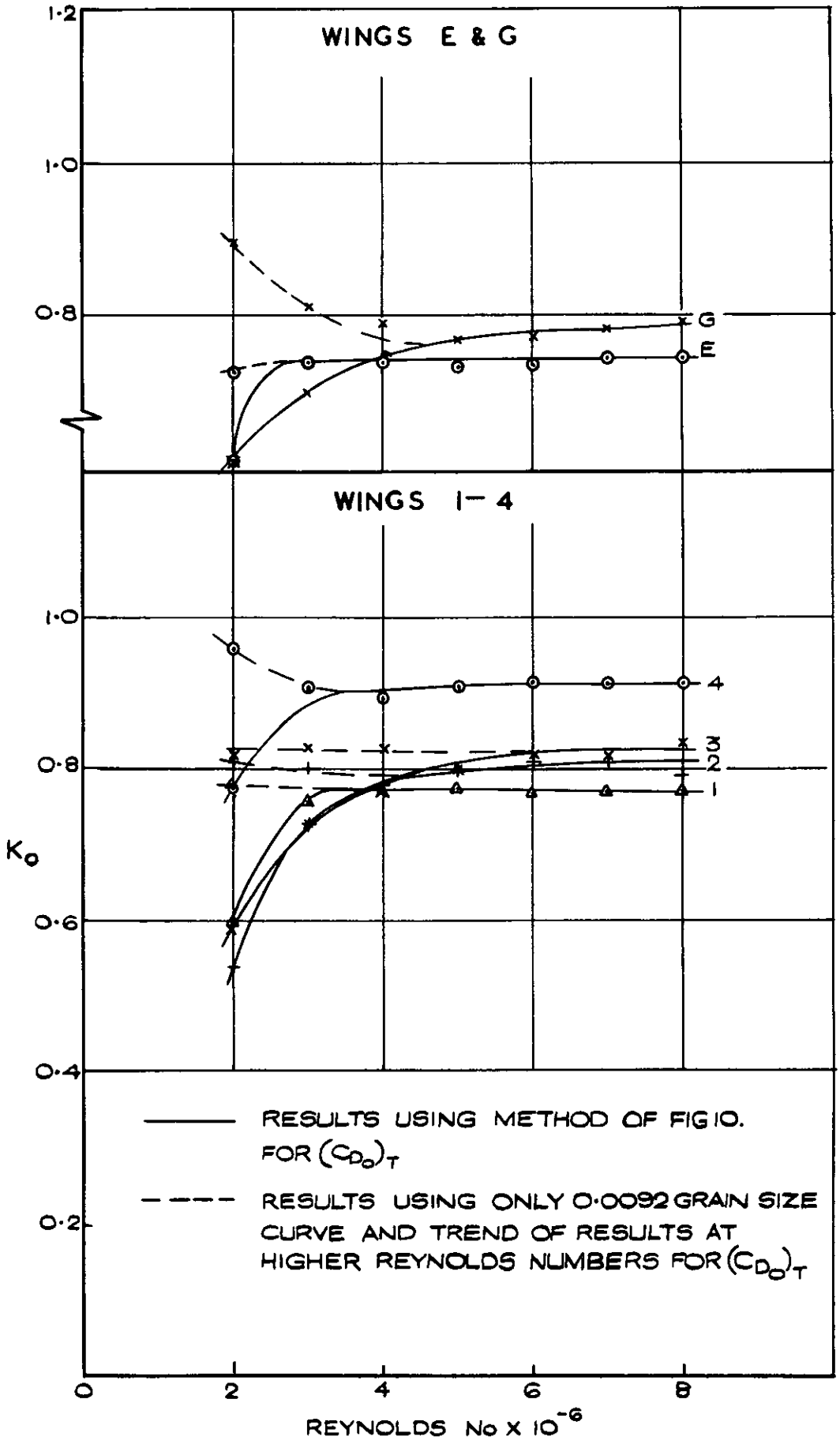

FIG. 17. DERIVED WAVE DRAG FACTORS (K_o) - M = 2·01.

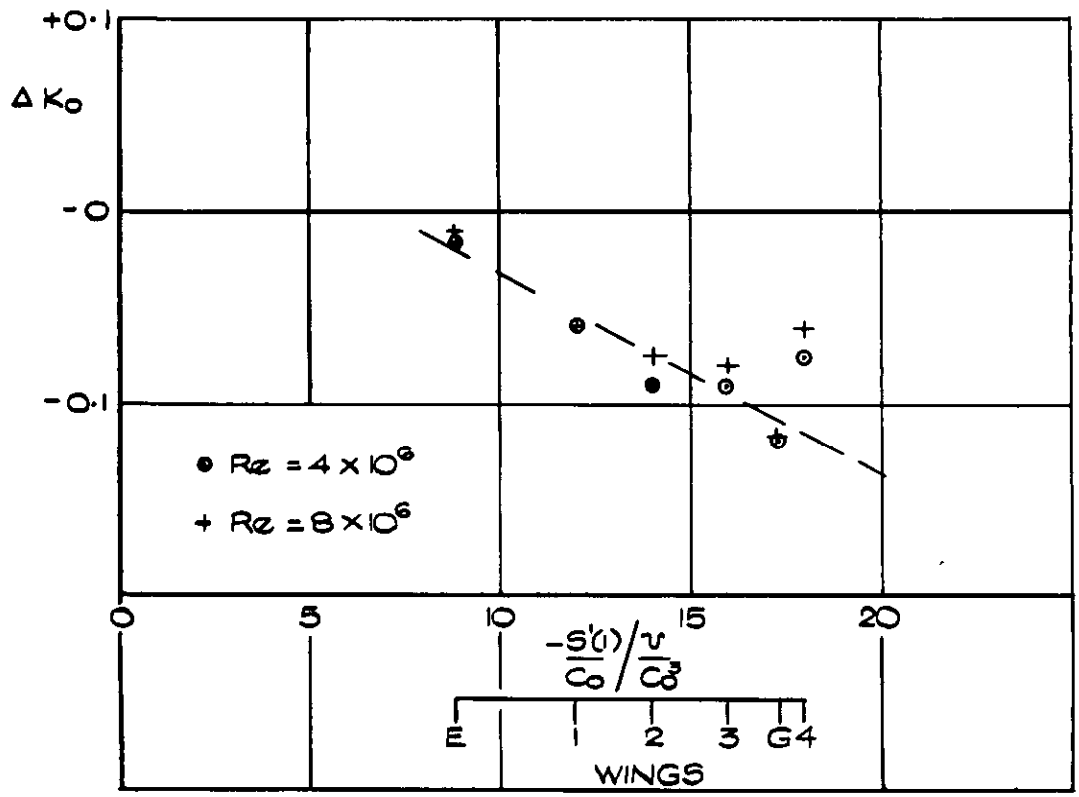

FIG. 18 ΔK_0 VERSUS $\frac{-S'(1)}{C_0} / \frac{\upsilon}{C_0^3}$ ALL WINGS M = 2·01.

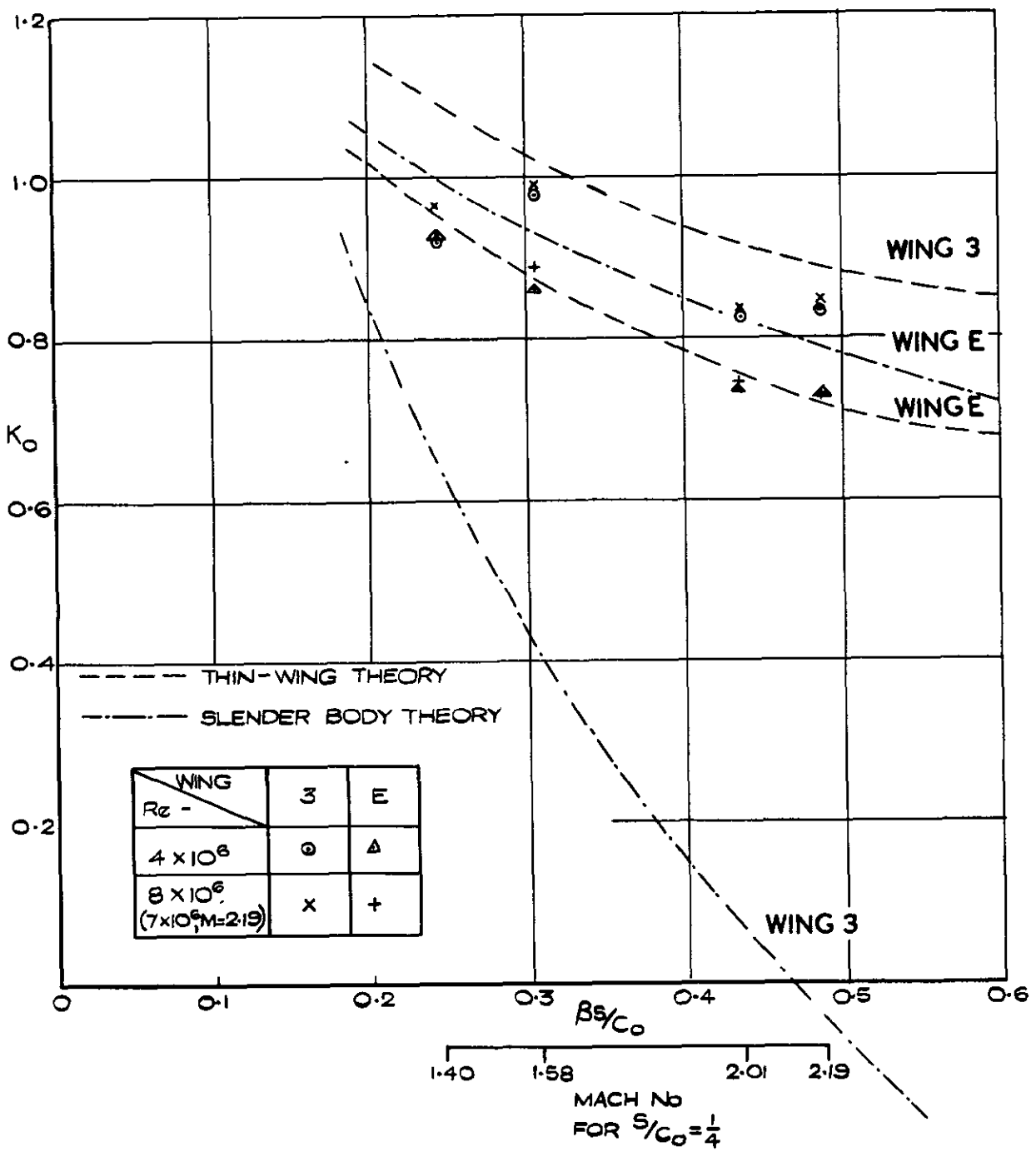

FIG.19. COMPARISON OF EXPERIMENTAL WAVE DRAG FACTORS WITH THIN-WING THEORY AND SLENDER BODY THEORY WINGS 3 AND E.

A.R.C. C.P. No. 737

533.693.3 :
533.6.013.12 :
533.6.011.5

EXPERIMENTAL EVIDENCE ON THE DRAG AT ZERO LIFT ON A SERIES OF SLENDER DELTA WINGS AT SUPERSONIC SPEEDS, AND THE DRAG PENALTY DUE TO DISTRIBUTED ROUGHNESS. Firmin, M.C.P. February, 1963.

Measurements have been made of the drag at zero lift on a series of low drag delta wings of diamond cross-section, with and without distributed roughness.

After allowance has been made for the skin friction, wave drag factors obtained have been compared with theoretical estimates. It is shown that thin-wing theory gives reasonably reliable estimates for the wave drag factor (K_o) but that it tends to overestimate the change in drag as the trailing edge slope is increased.

A.R.C. C.P. No. 737

533.693.3 :
533.6.013.12 :
533.6.011.5

EXPERIMENTAL EVIDENCE ON THE DRAG AT ZERO LIFT ON A SERIES OF SLENDER DELTA WINGS AT SUPERSONIC SPEEDS, AND THE DRAG PENALTY DUE TO DISTRIBUTED ROUGHNESS. Firmin, M.C.P. February, 1963.

Measurements have been made of the drag at zero lift on a series of low drag delta wings of diamond cross-section, with and without distributed roughness.

After allowance has been made for the skin friction, wave drag factors obtained have been compared with theoretical estimates. It is shown that thin-wing theory gives reasonably reliable estimates for the wave drag factor (K_o) but that it tends to overestimate the change in drag as the trailing edge slope is increased.

A.R.C. C.P. No. 737

533.693.3 :
533.6.013.12 :
533.6.011.5

EXPERIMENTAL EVIDENCE ON THE DRAG AT ZERO LIFT ON A SERIES OF SLENDER DELTA WINGS AT SUPERSONIC SPEEDS, AND THE DRAG PENALTY DUE TO DISTRIBUTED ROUGHNESS. Firmin, M.C.P. February, 1963.

Measurements have been made of the drag at zero lift on a series of low drag delta wings of diamond cross-section, with and without distributed roughness.

After allowance has been made for the skin friction, wave drag factors obtained have been compared with theoretical estimates. It is shown that thin-wing theory gives reasonably reliable estimates for the wave drag factor (K_o) but that it tends to overestimate the change in drag as the trailing edge slope is increased.

Slender body theory should not be relied upon to calculate the zero lift wave drag factors since in the region of the trailing edge the assumption of slenderness $\{|\beta^2\phi_{xx}| << |\phi_{yy}| + |\phi_{zz}|\}$ is only valid for a very restricted range of wings.

Slender body theory should not be relied upon to calculate the zero lift wave drag factors since in the region of the trailing edge the assumption of slenderness $\{|\beta^2\phi_{xx}| << |\phi_{yy}| + |\phi_{zz}|\}$ is only valid for a very restricted range of wings.

Slender body theory should not be relied upon to calculate the zero lift wave drag factors since in the region of the trailing edge the assumption of slenderness $\{|\beta^2\phi_{xx}| << |\phi_{yy}| + |\phi_{zz}|\}$ is only valid for a very restricted range of wings.

Published by
HER MAJESTY'S STATIONERY OFFICE

To be purchased from
York House, Kingsway, London w.c.2
423 Oxford Street, London w.1
13A Castle Street, Edinburgh 2
109 St. Mary Street, Cardiff
39 King Street, Manchester 2
50 Fairfax Street, Bristol 1
35 Smallbrook, Ringway, Birmingham 5
80 Chichester Street, Belfast 1
or through any bookseller

S.O. CODE No. 23-9015-37